Fall 10-31-1996

Modeling of cardiovascular system to simulate ventricular septal defect

Adarsh Kumar Gupta
New Jersey Institute of Technology

Copyright Warning & Restrictions

The copyright law of the United States (Title 17, United States Code) governs the making of photocopies or other reproductions of copyrighted material.

Under certain conditions specified in the law, libraries and archives are authorized to furnish a photocopy or other reproduction. One of these specified conditions is that the photocopy or reproduction is not to be "used for any purpose other than private study, scholarship, or research." If a, user makes a request for, or later uses, a photocopy or reproduction for purposes in excess of "fair use" that user may be liable for copyright infringement,

This institution reserves the right to refuse to accept a copying order if, in its judgment, fulfillment of the order would involve violation of copyright law.

Please Note: The author retains the copyright while the New Jersey Institute of Technology reserves the right to distribute this thesis or dissertation

Printing note: If you do not wish to print this page, then select "Pages from: first page # to: last page #" on the print dialog screen

ABSTRACT

MODELING OF CARDIOVASCULAR SYSTEM TO SIMULATE VENTRICULAR SEPTAL DEFECT

by

Adarsh Kumar Gupta

The hemodynamics of the ventricular septal defect is studied using a mathematical modeling technique. A twelve-compartment windkessel model of cardiovascular system is used to study the hemodynamics of the ventricular septal defect. The VSD is incorporated into the model via a parallel flow from the left to right ventricles (left-to-right shunt). The resistance to flow through the shunt is used to characterize the severity of the defect. Changes in the severity of the shunt flow produces changes in the ratio of pulmonary to systemic flow in the circulation. When the pulmonary to systemic flow ratio is more than 2:1, the defect is considered large based on current clinical guidelines. A safe-limit shunt hemodynamic resistance corresponding to a ratio of 2:1 was found to be 0.33 mmHg/ml/sec. This is high compared with the normal resistance of the pulmonary valve (0.0333 mmHg/ml/sec), mitral valve (0.0334 mmHg/ml/sec) and aortic valve (0.02 mmHg/ml/sec). The model also predicted that increasing pulmonary artery resistance reduces the work load on the heart.

Despite the simplicity of the model, the results showed good agreement with available clinical and experimental data. This model provides a useful basis for analyzing the hemodynamics of ventricular septal defects.

MODELING OF CARDIOVASCULAR SYSTEM TO SIMULATE VENTRICULAR SEPTAL DEFECT

by
Adarsh Kumar Gupta

A Thesis
Submitted to the Faculty of
New Jersey Institute of Technology
in Partial Fulfillment of the Requirements for the Degree of
Master of Science in Biomedical Engineering

Biomedical Engineering Committee

October 1996

APPROVAL PAGE

MODELING OF CARDIOVASCULAR SYSTEM TO SIMULATE VENTRICULAR SEPTAL DEFECT

Adarsh Kumar Gupta

Dr. Arthur Ritter, Thesis Advisor — Date
Professor of Physiology, New Jersey Medical School, UMDNJ

Dr. David Kristol, Committee Member — Date
Professor, Department of Biomedical Engineering, NJIT

Dr. Stanley Reisman, Committee Member — Date
Professor, Department of Electrical Engineering, NJIT

BIOGRAPHICAL SKETCH

Author: Adarsh Kumar Gupta

Degree: Master of Science

Date: October 1996

Undergraduate and Graduate Education:

- Master of Science in Biomedical Engineering,
  New Jersey Institute of Technology, Newark, NJ 1996
- Bachelor of Science in Chemical Engineering,
  New Jersey Institute of Technology, Newark, NJ 1995

Major: Biomedical Engineering

To my beloved family

ACKNOWLEDGMENT

I would like to express my deepest appreciation to Dr. Arthur Ritter, who not only served as my research advisor, provided valuable resources, and insight, but also gave me support, encouragement and reassurance. Special thanks to Dr. David Kristol and Dr. Stanley Reisman for actively participating on my committee.

TABLE OF CONTENTS

LIST OF TABLES

LIST OF FIGURES

LIST OF FIGURES
(Continued)

CHAPTER 1

INTRODUCTION

1.1 Physiology of Cardiovascular System

The cardiovascular system can be, conceptually, divided into the following functional components: blood, vessels, heart, and its associated control systems [7]. The functional anatomy of the cardiovascular system is shown in Figure 1.1.

1.1.1. Blood

Blood functions as the "carrier" for transporting substances to and from the various tissues. It also acts to remove noxious products from the cells, like carbon dioxide and metabolic wastes. It even removes excess heat from metabolizing tissues and transports it to the skin where it can be radiated into the environment. The circulating blood keeps the internal fluid matrix well stirred such that the most of the transport is by convection rather than by diffusion.

1.1.2. Blood Vessels

Blood vessels act to control blood flow to the tissues. The blood vessels serve as conduits to route the blood from the heart to the tissues. They have important regulatory functions as well. Blood is a viscous fluid constrained to move in a series of conduits having properties of resistance and compliance. By altering the properties of this plumbing system (circulatory system), the body can control the flow through any particular region of the cardiovascular system. This is accomplished by smooth muscles in the walls of the blood vessels which can alter the resistance and compliance as required.

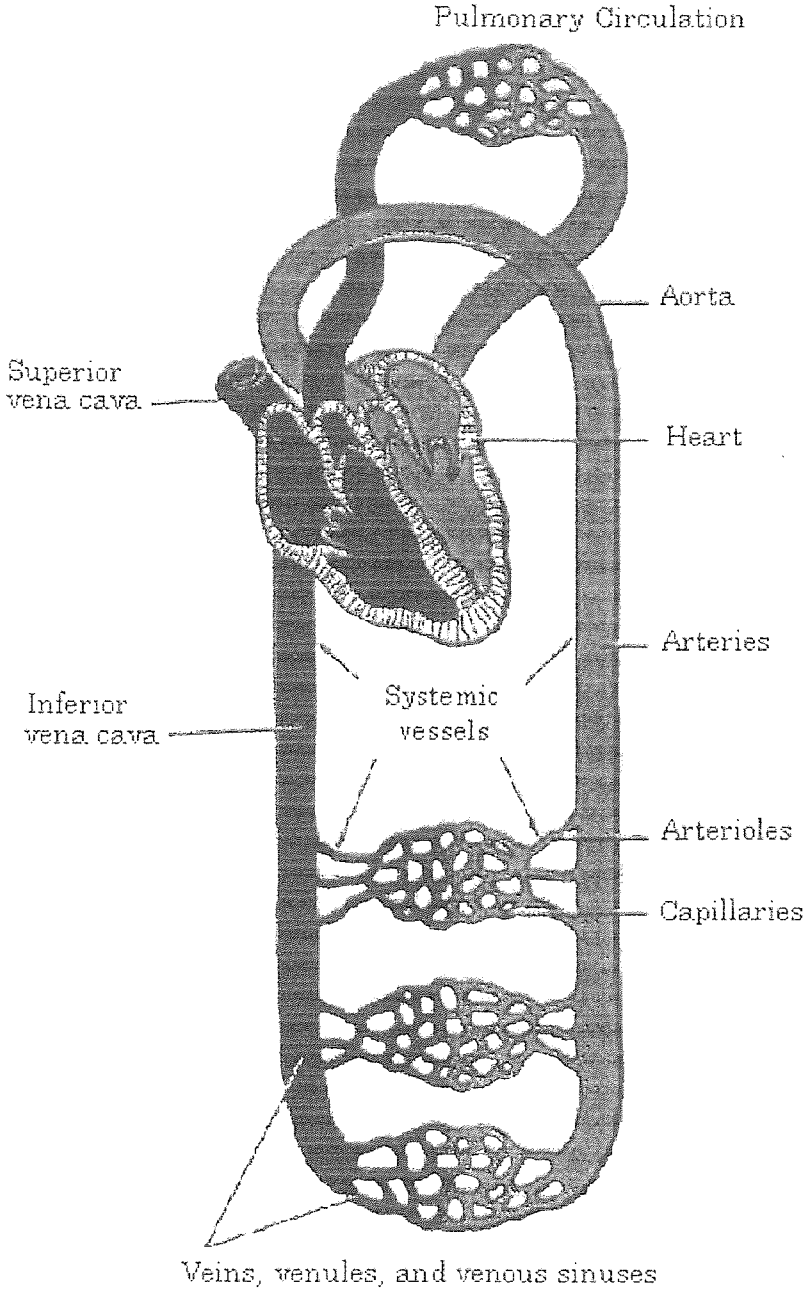

Figure 1.1 Cardiovascular System

The major components of cardiovascular system .i.o. heart, aorta, arteries, arterioles, systemic capillaries, veins, venules, inferior & superior vena cava, pulmonary capillaries and their arrangement in the system [5].

1.1.3. Heart

The heart is a hollow muscular organ that receives blood from the veins and propels it into and through the arteries. It acts as a reciprocating pump. The heart of a human is about the size of a closed fist. It is situated behind the lower part of the breastbone, extending more to the left of the midline than to the right. The heart is held in place principally by its attachment to the great arteries and veins, and by its confinement in the pericardium, a double-walled sac with one layer enveloping the heart and the other attached to the breastbone, the diaphragm, and the membranes of the thorax.

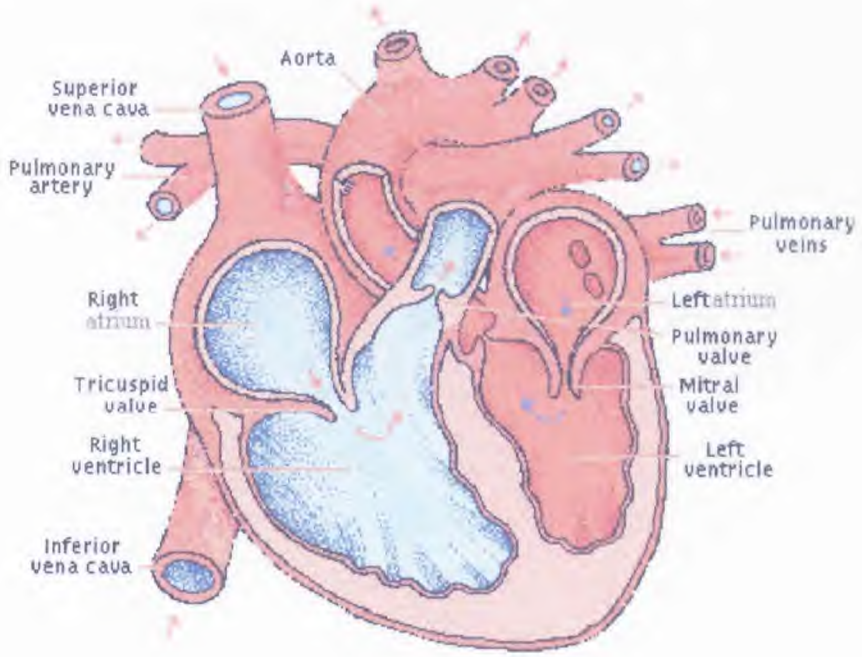

Figure 1.2. Human heart

The heart is a dual pump, circulating blood through two separate closed systems. Oxygen-carrying blood leaves the left ventricle through the aorta. It circulates through the body and returns, deoxygenated, to the right atrium via the superior and inferior vena cavae. The right ventricle pumps this blood through the pulmonary artery to the lungs, where it exchanges carbon dioxide for oxygen. Oxygenated blood then returns to the left atrium of the heart through the pulmonary veins ready for arterial circulation [Microsoft Encarta Illustration]

In the adult heart, there are two parallel independent systems, each consisting of an atrium and a ventricle; from their anatomical positions these systems are often designated the right heart and the left heart. The right heart propels blood through the pulmonary system, and the left heart propels blood through the systemic circulation. Since the two sides are in series the output of the left chamber must equal that of the right and that flow is termed the *cardiac output*.

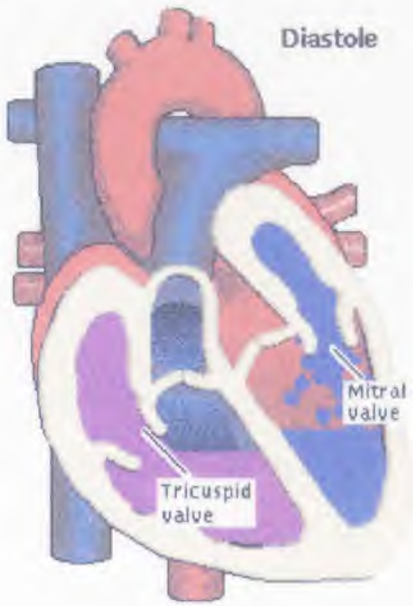

Figure 1.3a Diastole

Blood from the body returns to the right atrium through two large veins, the superior and inferior venae cavae; in addition the blood that has supplied the heart muscle is drained directly into the right atrium through the coronary sinus. Return of venous blood to the right atrium takes place during the entire heart cycle of contraction and relaxation, and to the right ventricle only during the relaxation part of the cycle, called *diastole*, when both right heart cavities constitute a common chamber; near the end of diastole, contraction of the right atrium completes the filling of the right ventricle with blood. Rhythmic contractions of the right ventricle expels the blood through the pulmonary

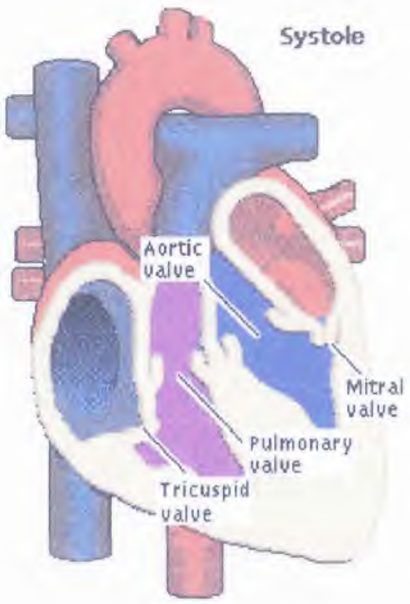

Figure 1.3b Systole

arteries into the capillaries of the lung, where the blood receives oxygen. The lung capillaries then empty into the pulmonary veins, which in turn empty into the left atrium.

Pulmonary venous return to the left atrium and left ventricle proceeds simultaneously in the same manner as the venous return to the right heart cavities. Contraction of the left ventricle rhythmically propels the blood into the aorta and from there to all arteries of the body, including the coronary arteries which supply the heart muscle.

The blood forced from the ventricles during *systole*, or contraction, is prevented from returning during diastole by valves at the openings of the aortic and pulmonary arteries. These valves consist of three semilunar (half-moon-shaped) flaps of membrane, which are curved in the direction of blood flow and which open readily on pressure in that direction; when the original pressure subsides, back pressure forces the edges of the flaps together. The tricuspid valve, situated between the right atrium and ventricle, is composed of three triangular flaps of membrane, and the bicuspid or mitral valve, between the left atrium and ventricle, has two such

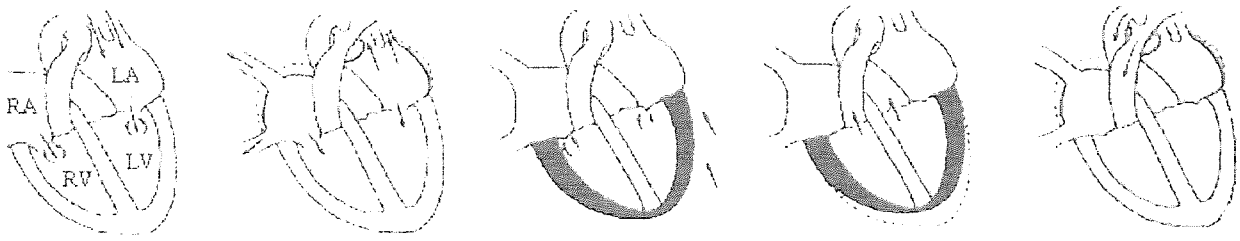

Figure 1.4. Blood Flow during a cardiac cycle.

Blood flow in the heart, great veins, aorta, and pulmonary arteries during a single cardiac cycle. Atrial and ventricular contractions are symbolized by shading the wall. Right and left atria are designated by RA and LA and right and left ventricles by RV and LV [7].

flaps. The bases of the flaps in both these valves are attached in a groove at the junction of the atrium and ventricle; the free edge is anchored by tendinous cords, known as the chordae tendinae, to the muscles of the heart wall. The flaps remain open until the ventricle fills with blood. When the ventricle begins to contract, the valve is closed by pressure. The chordae tendinae prevent inversion of the flaps during this period of systolic pressure.

Blood flow in the heart, great veins, aorta, and pulmonary arteries during a single cardiac cycle is shown in Figure 1.4.

1.2 Ventricular Septum Defect - Background

Ventricular septal defect (VSD) is the commonest congenital defect present at birth. The cardinal features of ventricular septal defect are left-to-right shunt into the right ventricle, increased pulmonary blood flow, and usually a low pulmonary artery pressure. Variable features are the size of the defect (large or small), the site of the defect (membranous or muscular), the level of the pulmonary vascular resistance, and the presence or absence of associated aortic incompetence. The size and site of the ventricular sepal defect determine the size of the left-to-right shunt, which in turn determines the clinical picture. A left-to-right shunt at the ventricular level produces an increased flow through the left atrium, left ventricle, and right ventricle. The right atrium is the only chamber through which flow is normal [4].

The anatomic location of ventricular septal defects are shown in Figure 1.5. Hemodynamic features of the ventricular septal defect is shown in Figure 1.6.

1.3 Objective and Purpose

The ventricular septal defect is an anomaly of the septum which mostly occurs in early childhood. Children who have *small defects* and shunts are well developed and asymptomatic. *Large defects* may cause symptoms in early infancy. Growth failure is usual in such cases; weight gain may be distressingly slow, and the children are pale, delicate -looking, and scrawny. Feeding difficulties, respiratory infections, and congestive failures are common, and the infants may spend more time in hospital

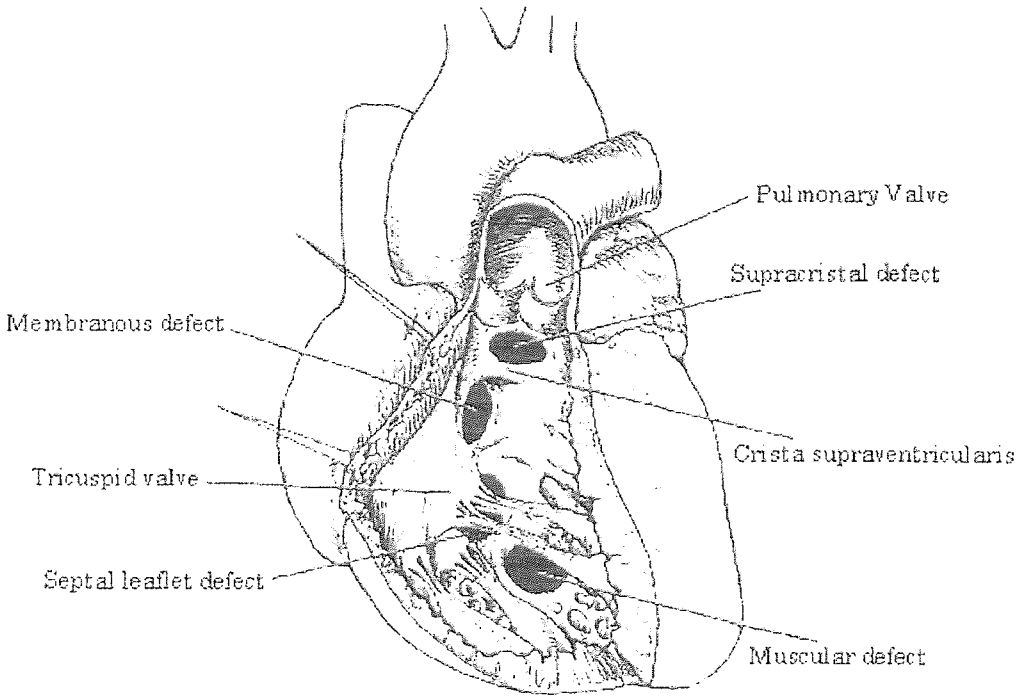

Figure 1.5. Ventricular Septal Defect

Anatomic location of ventricular septal defects. *Cardinal features:* Left-to-right shunt into right ventricle; increased pulmonary blood flow; pulmonary arterial pressure usually low. *Variable features:* Size of defect; site of defect: membranous or muscular; associated aortic incompetence [4].

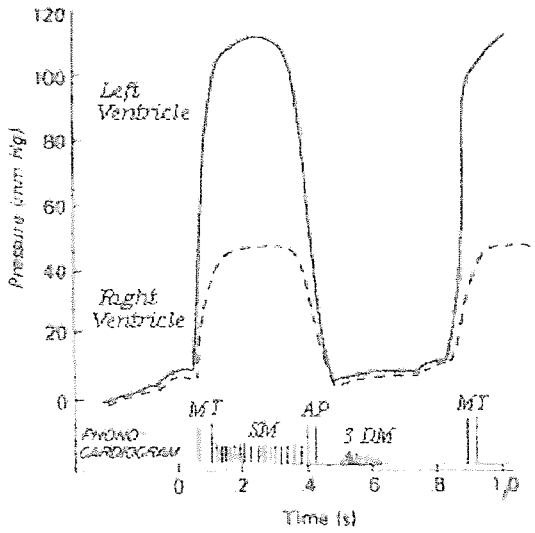

Figure 1.6. Hemodynamics of Ventricular Septal Defect

Diagram showing ausculatory and hemodynamic features of ventricular septal defect. M, mitral; T, tricuspid; SM, systolic murmur; A, aortic; P, pulmonary; DM, diastolic murmur [4].

than at home (Netter, F.H.). In such a situation, it is conceivable that an optimum patient management program could be devised, if various hemodynamic parameters and probable factors responsible for the disease could be identified. It is not possible to do such a study for hemodynamic parameters and factors in humans (children), and there is no animal model of VSDs. Thus, mathematical modeling and computer simulation are attractive methods for study of this problem. Simulation is a flexible tool allowing change of parameters and control of variables while reducing animal and human experimentation. It can extrapolate from known states to those projected states that cannot be measured directly and to approximate those variables that are inaccessible to experiment.

Fortunately, many aspects of the structure and function of the cardiovascular system can be described and analyzed in mathematical terms. In the present study, a mathematical model of the closed-loop cardiovascular system was devised. The

Ventricular Septal Defect was then incorporated into the model to study the effect of cardinal and variable features of the disease on the hemodynamics of the heart.

1.4 History of Mathematical Modeling of Cardiovascular System

Model studies of overall cardiovascular system involving a closed loop with constancy of total blood volume originate from Guyton (1955), who used the fact that venous return and cardiac output must be equal when the circulatory system is in a steady state [2].

Grodins (1959) published a compartmental study of the cardiovascular system based on twenty-three independent simultaneous equations, the solution of which gave mean values for the variables. Cardiac activity was represented by a linear relation between end-diastolic ventricular volume and stroke work. The results from this model compare favorably with those of physiologic experiments [2].

Warner (1959) used six compartments to represent the circulatory system. A total of 18 equations were needed for the solution which also included the pulsatile character of the variables. Ventricular contraction and relaxation were represented by compliance changes. In 1963, Defares *et al.* published an extensive mathematical description of the entire uncontrolled system. [2].

The long term model devised by Guyton and Coleman (1967) is original and it incorporates not only immediate baroreceptor action but also its long-term adaptation. Cardiac output is determined by the strength of the heart, vascular resistance and blood volume. Vascular resistance was determined by autoregulation of blood flow with above-normal cardiac output causing vasoconstriction and below-normal cardiac output causing vasodilatation [2].

Currently, more complex and realistic models have been developed which model many aspects of the cardiovascular system in great detail. These published models of the cardiovascular system are being used for different research projects.

CHAPTER 2

MATHEMATICAL MODEL OF CARDIOVASCULAR SYSTEM

2.1 Model Concept and Assumptions

The model of the cardiovascular system which is used in this work is composed of twelve compartments (Figure 2.1) : left heart, aorta, large arteries, arterioles, systemic capillaries, venules, large veins, vena cava, right heart, pulmonary artery, pulmonary capillaries, and pulmonary vein. Each compartment consists of a characteristic resistance (R) and a compliance (C).

The following assumptions have been used in developing the present model:

1. The physical parameters of the system are linear, and can be lumped.
2. Blood flow within each area is influenced only by:
    a. Resistance, and
    b. Compliance
3. There is no resistance to blood flow between areas.

The relationship between blood flow and blood pressure in any compartment is given by:

$$F_n = \frac{P_n - P_{n+1}}{R_n} \tag{2.1.1}$$

where F_n is the blood flow out of n^{th} compartment and into compartment n+1. R_n is the resistance of the n^{th} compartment. P_n and P_{n+1} are the blood pressures of the compartment n and n+1.

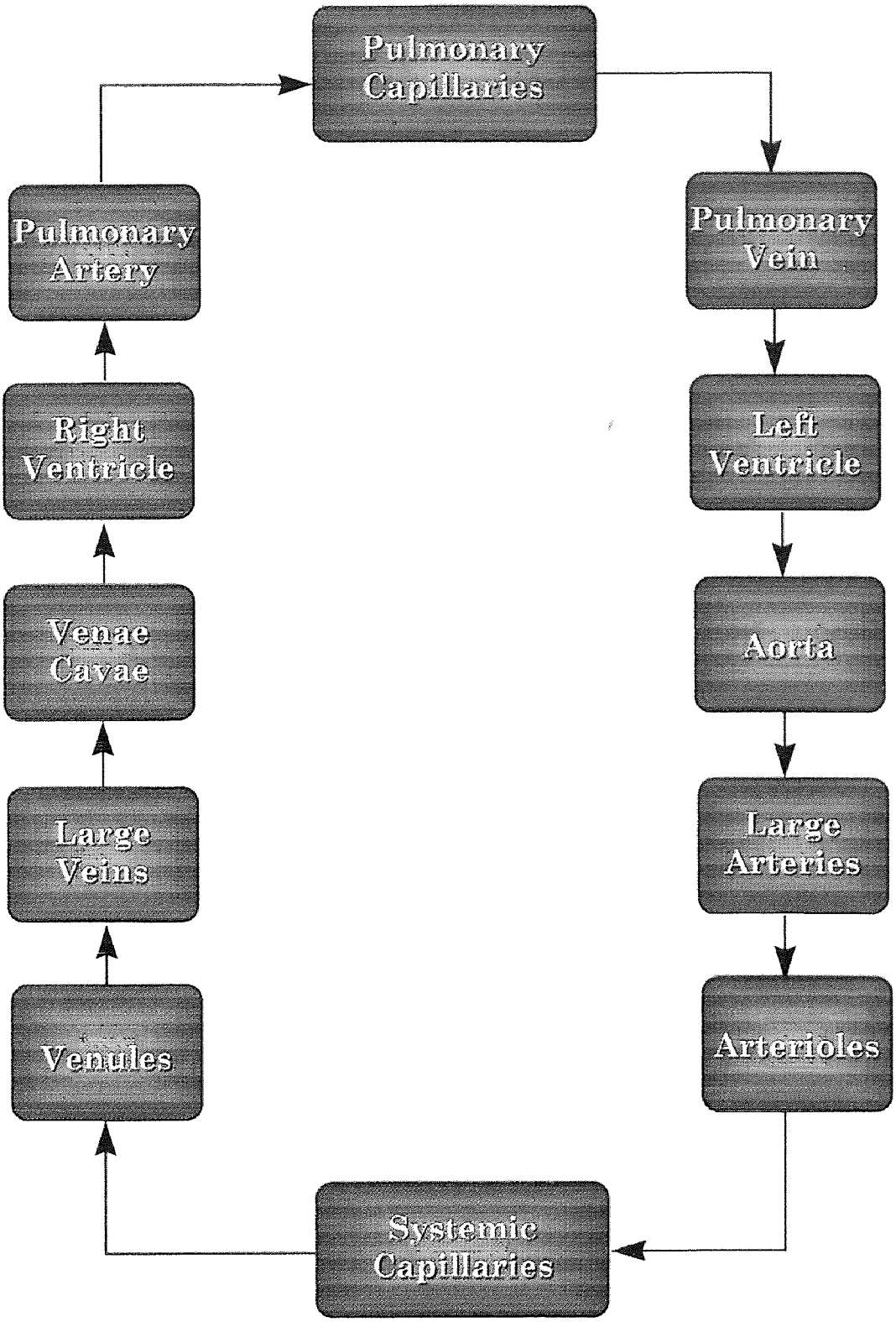

Figure 2.1 Cardiovascular Model

Block diagram representation of the cardiovascular system simulated in the present study.

The relationship between blood volume and blood pressure in a compartment is given by:

$$P_n = \frac{V_n - V_{n0}}{C_n} \tag{2.1.2}$$

where,

P_n is the blood pressure in n^{th} compartment

C_n is the compliance of n^{th} compartment.

V_n is the total blood volume in n^{th} compartment

V_{n0} is the unstressed blood volume in n^{th} compartment, that is, the volume when transmural pressure is zero. They are assumed known.

The total blood volume in a compartment can be represented by

$$V_n = V_{n0} + \int \left(F_{n-1} - F_n \right) \tag{2.1.3}$$

where,

F_{n-1} is the blood flow in compartment $n-1$.

F_n is the blood flow in n^{th} compartment.

The ventricles are represented by a Suga-Sagawa "varying elastance" model [16]. In this "varying elastance" model, the time-varying ratio of the pressure to volume at any instant is used to represent the pressure-volume relationship of the left ventricle in the dog. This pressure-volume ratio was defined as the elastance $E(t)$, which is represented by a normalized function $E_N(t)$ multiplied by its maximum value E_{max}, which is the peak value of the pressure-volume ratio curve (Figure 2.2). T_{max} is the time corresponding to E_{max} in the curve. According to their study, the contractility of the ventricles can be fully represented by these two parameters, E_{max} and T_{max}.

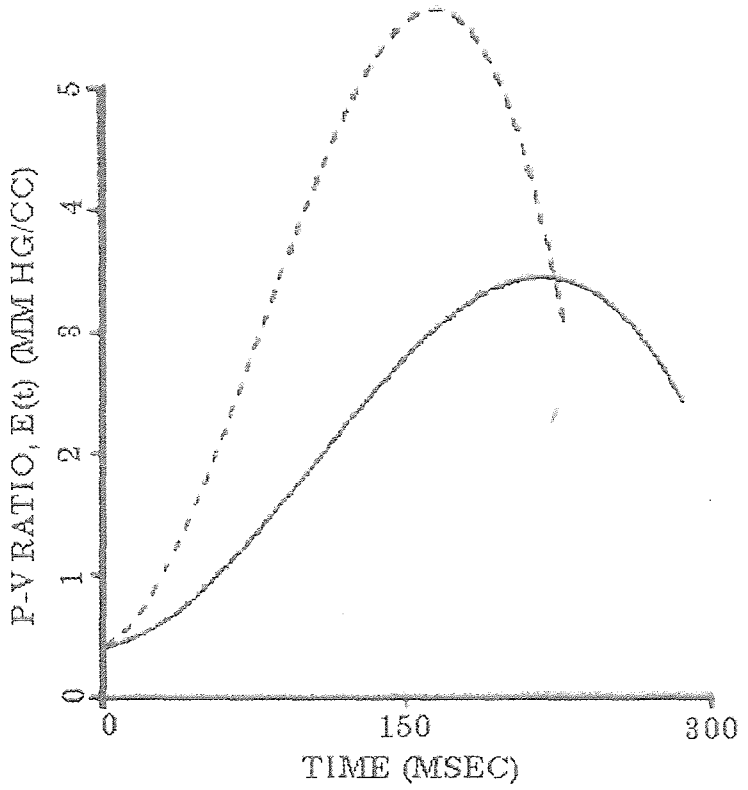

Figure 2.2. Time-varying pressure-volume ratio, E(t).

Time-varying pressure-volume ratio, E(t), of the left ventricle for the control contractile state (solid line) and the enhanced contractile state (dash line).

Therefore, the intraventricular pressure-volume relationship can be represented as follows:

$$P_{lv}(t) = E_{lv}(t) \times \left(V_{lv}(t) - V_{lvo}\right) \qquad (2.1.4a)$$

where,

$E_{lv}(t)$ is the elastance of left ventricle.

V_{lv0} is the volume axis intercept of the line connecting the maximum left ventricular elastance P/V points for different loaded beats, which is a constant.

The elastance of the left ventricle can be expressed as:

$$E_{lv}(t) = E_{l\max} E_N(t / T_{\max}) \qquad (2.1.5a)$$

where,

E_{lmax} is the maximum value of $E_{lv}(t)$.

$E_N(t)$ is the normalized elastance and is represented by

$$E_N(t) = \sum_{n=1}^{3} a_n t^n T_{\max}^{-n} \qquad (2.1.6)$$

where the coefficients a_1, a_2, and a_3 are the parameters used by Shroff *et al.* [14] and Barnea *et al.*[1] in their model for $E_N(t)$. These are given as follows:

$a_1 = 0.158$, $a_2 = 2.685$, $a_3 = -1.841$

T_{max} is the time at which the $E_{lv}(t)$ reaches the maximum value E_{max} from the onset of systole. It can be calculated as follows:

$$T_{\max} = \frac{(413 - 1.7 \times HR)}{100} \qquad (2.1.7)$$

where HR is in beats per minute, T_{max} is in seconds.

The right ventricular elastance model is similar to that of left ventricle except that it has different $E_{rv}(t)$ and E_{rmax} is about one-fifth of E_{lmax}. The right ventricular pressure is represented as follows:

$$P_{rv}(t) = E_{rv}(t) \times \left(V_{rv}(t) - V_{rvo}\right) \qquad (2.1.4b)$$

$$E_{rv}(t) = E_{r\max} E_N(t / T_{\max}) \qquad (2.1.5b)$$

where,

V_{rv0} is the volume axis intercept of the line connecting the maximum right ventricular elastance P/V points for different loaded beats. It is assumed constant in this model.

During diastole, the compliance of the ventricles are assumed constant, but the left ventricle has a different value than the right ventricle.

2.2 Hemodynamics and System Parameters

Hemodynamics refers to the physics that governs blood flow within the cardiovascular system. In its simplest form the cardiovascular system can be considered to be a pump, the heart, in series with a system of tubes through which it pumps blood.

Cardiac hemodynamics can be represented by two types of variables:

1. *Cardiovascular parameters*, which characterise the mechanical property of a particular part of the system, such as vascular resistance and capacitance, ventricular contractility and stiffness.
2. *Hemodynamic variables*, such as cardiac output, blood pressure and volume in each compartment, which are determined wholly in the circulation as a function of cardiovascular parameters.

Most of the hemodynamic variables can be measured directly. For example, cardiac output can be measured by using the direct Fick method or by the indicator dilution technique, left ventricular volume can be measured using angiocardiograms, intracardiac pressures can be measured using cardiac catheterization techniques.

However, many of the cardiovascular parameters, such as vascular compliance and ventricular contractility, are difficult to measure directly. The values of these independent parameters are usually determined by

(a) measuring experimentally if possible,

(b) estimating from measured data with appropriate assumptions, and

(c) assuming a reasonable constant value.

Furthermore, these parameters are often additionally tuned to achieve a good match with a wide range of known data.

In the present study, the value for the hemodynamic variables were all chosen from data published in the literature. The values for the cardiovascular parameters were estimated with as few assumptions as possible because there is no standard set of values available for them. Ventricular elastance was based on the "variable elastance" model of Suga. Hemodynamic resistance and compliance were estimated from blood flow, pressure and volume data.

The blood pressure changes in a normal human at rest in various portions of the circulatory system are shown in Figure 2.3. The parameters and variables used in the present model for a normal human at rest, are listed in Table 2.1

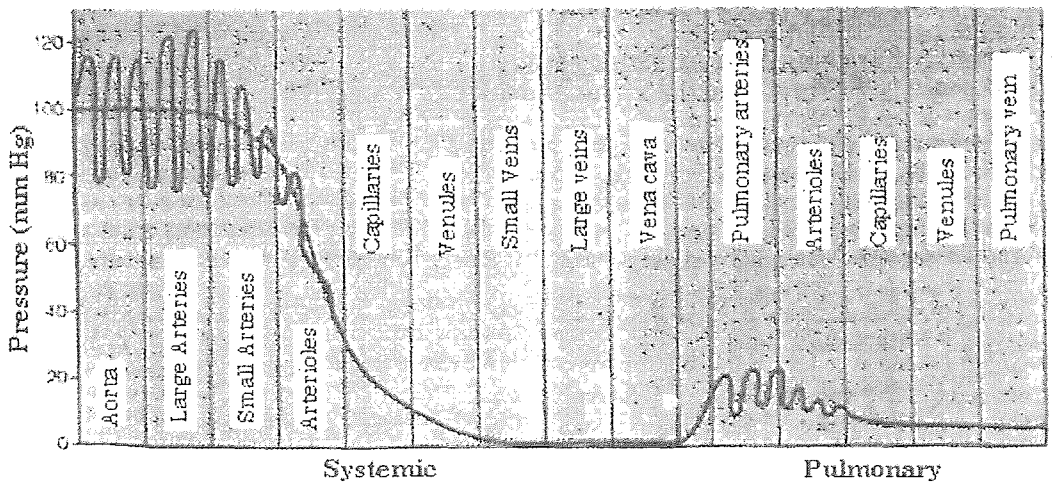

Figure 2.3. Pressures in various portions of circulation

Blood pressure in the different portions of the circulatory system.

Table 2.1. Standard values of variables and parameters used in the present model for a normal human at rest.

	Resistance (R) (mm Hg /ml/sec)	Compliance (C) (ml/mm Hg)	Unstressed Volume, V_0 (ml)
Left Heart	IN: **0.0334** OUT: **0.02**	**2 - 0.051**	**0**
Aorta	**0.0944**	**0.625**	**60**
Large Arteries	**0.1307**	**0.725**	**58**
Arterioles	**0.8499**	**1.667**	**52.9**
Systemic Capillaries	**0.0567**	**15**	**270.0**
Venules	**0.0056**	**20.5**	**278.1**
Large Veins	**0.0283**	**121.5**	**1586.4**
Vena Cava	**0**	**21.5**	**300.5**
Right Heart	IN: **0.0069** OUT:**0.0333**	**0.45 - 0.048**	**10**
Pulmonary Artery	**0.025**	**5**	**87.5**
Pulmonary Capillaries	**0.02**	**4.44**	**67.5**
Pulmonary Vein	**0**	**7.9**	**146.5**

For a normal human, **Heart Rate = 75 beats/min**

2.3 Mathematical Model - Equations

In general, each compartment of the present cardiovascular model consists of following equations:

$$F_n = \frac{P_n - P_{n+1}}{R_{n+1}} \tag{2.1.1}$$

$$P_n = \frac{V_n - V_{n0}}{C_n} \tag{2.1.2}$$

$$V_n = V_{n0} + \int (F_{n-1} - F_n) \tag{2.1.3}$$

The equation for each compartment is shown below:

1. ***Left Heart***

FPvein =(*PPvein* - *PLV*) / (*RLVin*)

If *PPvein* < *PLV*, then *RLVin* = ∞ else *RLVin* = 0.0334 [Mitral Valve]

FLV = (*PLV* - *PAO*) / (*RLVout*)

If *PLV* < *PAO*, then *RLVout* = ∞ else *RLVout* = 0.02 [Aortic Valve]

PLV = (*VLV*-*VLo*) x $E_{lv}(t)$

$$VLV = VLo + \int (FPvein - FLV)$$

where, *FPvein* and *FLV* are the flows from pulmonary vein to left ventricle and from left ventricle to aorta, respectively. *PPvein*, *PLV*, and *PAO* are the pressure in the pulmonary vein, left ventricle and the aorta respectively. *VLV* is the volume of the left ventricle. $E_{lv}(t)$ is the elastance of the left ventricle and its plot is shown in Figure 2.4. During systole, $E_{lv}(t) = 2\ E_N(t)$ and during diastole, $E_{lv}(t) = 0.051$.

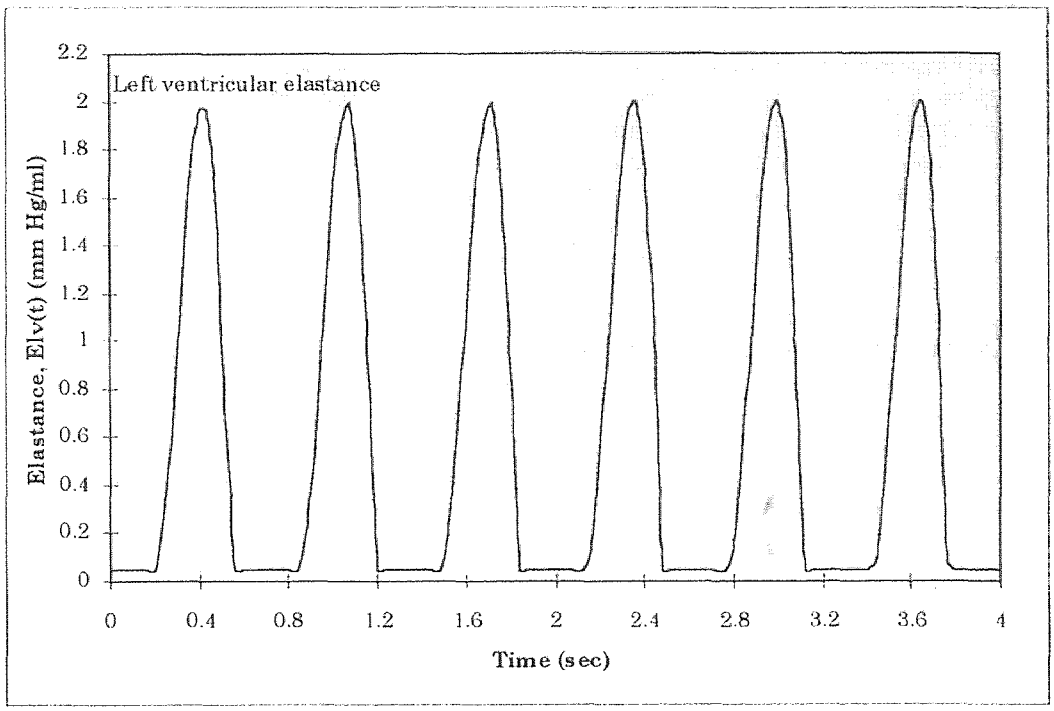

Figure 2.4. Elastance of Left Ventricle, $E_{lv}(t)$ vs. Time, t.

Elastance of left ventricle generated by the model for a normal human at rest, $E_{lv}(t)$.

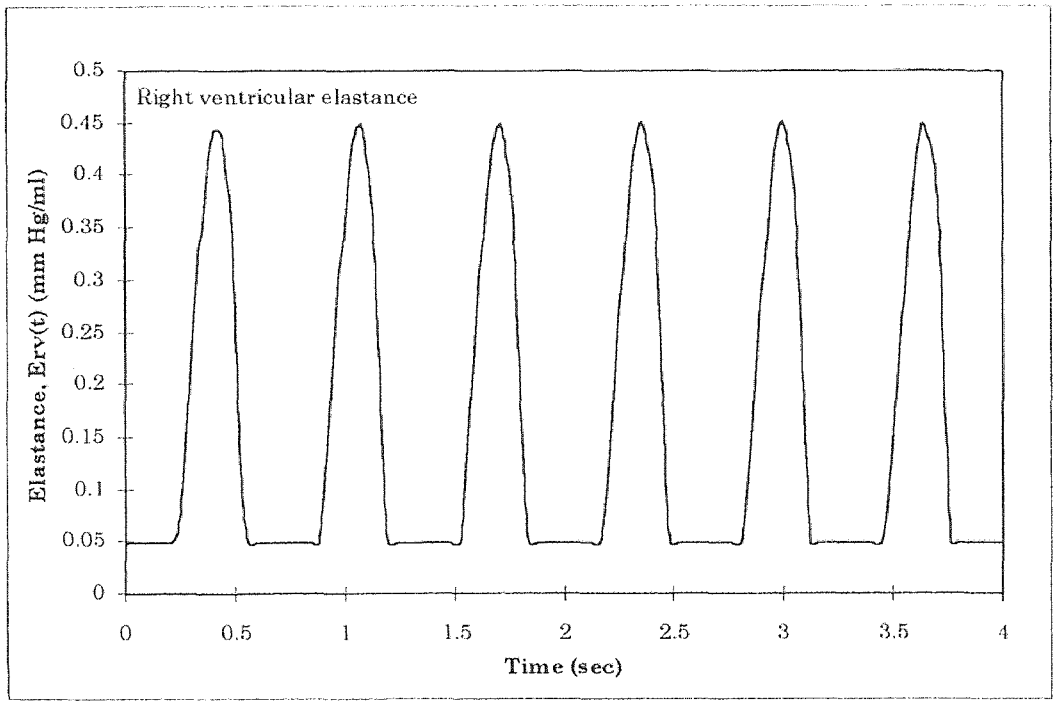

Figure 2.5. Elastance of Right Ventricle, $E_{rv}(t)$ vs. Time, t.

Elastance of right ventricle generated by the model for a normal human at rest, $E_{rv}(t)$.

2. ***Aorta***

$FAO = (PAO - PLart) / 0.0944$

$PAO = (VAO - 60) / 0.625$

$VAO = 60 + \int (FLV - FAO)$

where FAO is the flow from aorta to large arteries, $PLart$ is the pressure in large arteries. VAO is the volume of the aorta.

3. ***Large arteries***

$FLart = (PLart - Parteriol) / 0.1307$

$PLart = (VLart - 58) / 0.725$

$VLart = 58 + \int (FAO - FLart)$

where $FLart$ is the flow from large arteries to arterioles, $Parteriol$ is the pressure in arterioles. $VLart$ is the volume of large arteries.

4. ***Arterioles***

$Farteriol = (Parteriol - PScap) / 0.84997$

$Parteriol = (Varteriol - 52.9) / 1.667$

$Varteriol = 52.9 + \int (FLart - Farteriol)$

where $Farteriol$ is the flow from arterioles to systemic capillaries, $PScap$ is the pressure in systemic capillaries. $Varteriol$ is the volume of arterioles.

5. ***Systemic Capillaries***

$FScap = (PScap - Pvenule) / 0.0566$

$PScap = (VScap - 270.0) / 15$

$VScap = 270.7 + \int (Farteriol - FScap)$

where *FScap* is the flow from systemic capillaries to venules. *Pvenule* is the pressure in the venules. *VScap* is the volume of the systemic capillaries.

6. ***Venules***

$Fvenule = (Pvenule - PLvein) / 0.00566$

$Pvenule = (Vvenule - 278.1) / 20.5$

$Vvenule = 278.1 + \int (FScap - Fvenule)$

where, *Fvenule* is the flow from venules to large veins. *PLvein* is the pressure in large veins. *Vvenule* is the volume of the venules.

7. ***Large Veins***

$FLvein = (PLvein - Pvcava) / 0.02833$

$PLvein = (VLvein - 1586.4) / 121.5$

$VLvein = 1586.4 + \int (Fvenule - FLvein)$

where, *FLvein* is the flow from large veins to vena cava. *Pvcava* is the pressure in vena cava. *VLvein* is the volume of the large veins.

8. ***Vena Cava***

$Pvcava = (Vvcava - 300.5) / 21.5$

$Vvcava = 300.5 + \int (FLvein - Fvcava)$

where, *Vvcava* is the volume of vena cava.

9. ***Right Heart***

$Fvcava = (Pvcava - PRV) / RRVin$

If $Pvcava < PRV$, then $RRVin = \infty$ else $RRVin = 0.00689$

$FRV = (PRV - PPart) / RRVout$

If $PRV < PPart$, then $RRVout = \infty$ else $RRVout = 0.0333$

$PRV = (VRV - VRo) \times E_{rv}(t)$

$VRV = VRo + \int (Fvcava - FRV)$

where *Fvcava* and *FRV* are the flows from vena cava to right ventricle and from right ventricle to pulmonary artery, respectively. *Pvcava, PRV,* and *PPart* are the pressure in the vena cava, right ventricle and the pulmonary artery respectively. *VRV* is the volume of the right ventricle. $E_{rv}(t)$ is the elastance of the right ventricle and its plot is shown in Figure 2.5. During systole, $E_{rv}(t) = 0.45\ E_N(t)$ and during diastole, $E_{rv}(t) = 0.048$.

10. *Pulmonary Artery*

$FPart = (PPart - PPcap) / 0.025$

$PPart = (VPart - 87.5) / 5$

$VPart = 87.5 + \int (FRV - FPart)$

where *FPart* is the flow from pulmonary artery to pulmonary capillaries. *PPcap* is the pressure in pulmonary capillaries. *VPart* is the volume of the pulmonary artery.

11. *Pulmonary capillaries*

$FPcap = (PPcap - PPvein) / 0.02$

$PPcap = (VPcap - 67.5) / 4.44$

$VPcap = 67.5 + \int (FPart - FPcap)$

where *FPcap* is the flow from pulmonary capillaries to pulmonary vein. *PPvein* is the pressure in pulmonary vein. *VPcap* is the volume of the pulmonary capillaries.

12. *Pulmonary vein*

$PPvein = (VPvein - 146.5) / 7.9$

$VPvein = 146.5 + \int (FPcap - FPvein)$

where *VPvein* is the volume of the pulmonary vein.

Thus, the pulmonary vein completes the closed-loop cardiovascular model.

CHAPTER 3

MODEL OF VENTRICULAR SEPTAL DEFECT

3.1 Overall Concept

The ventricular septum is derived from three components: the muscular septum which arises from the ventricular walls, the membranous septum which arises from the atrioventricular cushions and grows down to meet the muscular septum, and the bulbar septum which separates the bulbus cordis into the outflow tracts of the right and left ventricles (Figure 3.1) [8].

The cardiovascular effects of a ventricular septal defect depends upon its size, the age of the patient and on the resistance to blood flow imposed by the pulmonary arterial vessels. If the defect is small, the jet of blood from the high-pressure left ventricle to the low-pressure right ventricle has little hemodynamic effect and is compatible with normal life expectancy. If the defect is large and the resistance of the pulmonary vessels low, a large shunt develops and the pulmonary blood flow can become more than twice as large as the systemic blood flow. Large defects with flow ratios of 3:1 or more are rare in adults and are usually associated with dyspnea on exertion [4].

The conventional methods of hemodynamic assessment of ventricular septal defect (VSD) are well known. They pertain to the measurement of pressure and oxygen, the latter as saturation, content, or partial pressure. They include the calculation of systemic, pulmonary, and effective flow, and of pulmonary and systemic vascular resistance, either in mutual relation or absolute figures [18].

The ECG in small defects is normal. When the left-to-right shunt is large there is usually biventricular hypertrophy, manifested by tall R waves, deep S waves over the transitional zone leads and Q waves in the left ventricular leads.

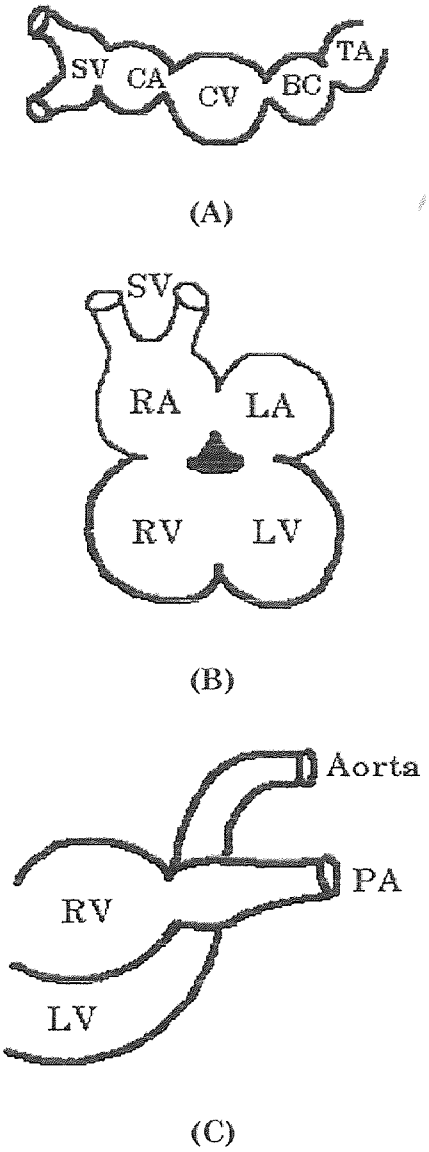

Figure 3.1. Ventricular Septal Defect Development
(A). The heart at the fourth week of pregnancy, divided by constrictions into sinus venosus (SV), common atrium (CA), common ventricle (CV), bulbus cordis (BC) and truncus arteriosus (TA). **(B)**. The heart at 8 weeks. The ventricles and atria are each being divided by septa into two chambers. Endocardial cushions develop from which the mitral and tricuspid valves are formed. **(C)**. The spiral septum divides the bulbus cordis into the outflow tracts of the left and right ventricles, and the truncus arteriosus into aorta and pulmonary arteries [4].

The chest radiograph is normal with a small defect, but with a large left-to-right shunt there is some enlargement of the heart and, more specifically, prominence of the pulmonary vessels, left atrium and both ventricles. Cardiac catheterization is indicated to confirm the diagnosis, especially if surgical treatment is contemplated [4].

3.2 Model of Left-to-right Shunt in VSD

The size of the left-to-right shunt is the cardinal feature of ventricular septal defect which is usually used to express the severity of the defect. In the present study, the same cardinal feature is used to model ventricular septal defect [15].

The left-to-right shunt (L-to-R) is the flow from the left ventricle to the right ventricle against the pressure gradient between the left ventricle and right ventricle. A larger value for L-to-R shunt flow indicates a large defect, and smaller values indicate smaller defects. The values for L-to-R shunt flows are directly related to the pulmonary and systemic blood flow [15] and is computed as:

Left-to-right shunt flow = Pulmonary blood flow - Systemic blood flow

The ratio of the pulmonary to systemic flow is often used to express the severity of the shunt. For example, if the pulmonary flow is 10 liter/min and the systemic flow is 5 liter/min, the magnitude of the shunt would be 2:1. The severity of shunt is computed as follow:

Severity of shunt = Pulmonary blood flow / Systemic blood flow

In the present study, the resistance of the L-to-R shunt is calculated at various severity levels of the shunt, i.e. at different pulmonary to systemic flow ratios to identify the safe-limit resistance of the L-to-R shunt.

3.3 Mathematical Model for VSD

The ventricular septal defect is incorporated into the existing cardiovascular model as another compartment connecting the left heart to right heart as shown in Figure 3.2. The model equations for the ventricular septal defect are similar to that of the existing cardiovascular model except the equations for the left and right heart compartment have been modified to incorporate the ventricular septal defect.

The model is represented as follow:

Left Heart:

$FPvein = (PPvein - PLV) / (RLVin)$

If $PPvein < PLV$, then $RLVin = \infty$ else $RLVin = 0.0334$ [Mitral Valve]

$FLV = (PLV - PAO) / (RLVout)$

If $PLV < PAO$, then $RLVout = \infty$ else $RLVout = 0.02$ [Aortic Valve]

$PLV = (VLV - VLo) \times E_{lv}(t)$

$$VLV = VLo + \int (FPvein - FLV - LtoRShunt)$$

where, $FPvein$, FLV and $LtoRShunt$ are the flows from pulmonary vein to left ventricle, from left ventricle to aorta, and from left ventricle to the right ventricle respectively. $PPvein$, PLV, and PAO are the pressure in the pulmonary vein, left ventricle and the aorta respectively. VLV is the volume of the left ventricle. $E_{lv}(t)$ is

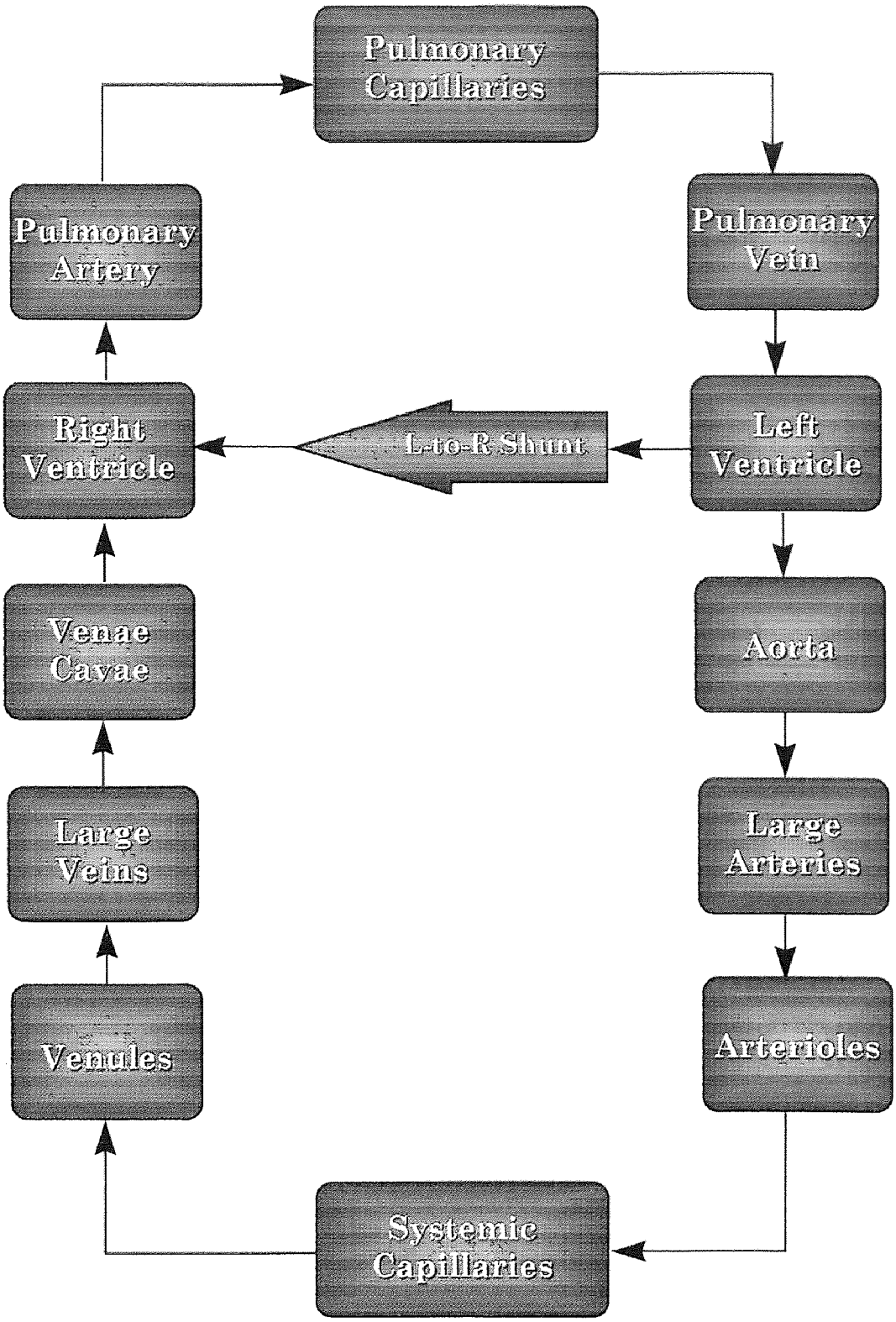

Figure 3.2. VSD Model.

Closed-loop lumped model of cardiovascular system with ventricular septal defect.

the elastance of the left ventricle and its plot is shown in Figure 2.4. During systole, $E_{lv}(t) = 2\ E_N(t)$ and during diastole, $E_{lv}(t) = 0.051$.

Right Heart:

$Fvcava = (Pvcava - PRV) / RRVin$

If $Pvcava < PRV$, then $RRVin = \infty$ else $RRVin = 0.00689$

$FRV = (PRV - PPart) / RRVout$

If $PRV < PPart$, then $RRVout = \infty$ else $RRVout = 0.0333$

$PRV = (VRV - VRo) \times E_{rv}(t)$

$$VRV = VRo + \int (Fvcava - FRV + LtoRShunt)$$

where $Fvcava$, FRV and $LtoRShunt$ are the flows from vena cava to right ventricle, from right ventricle to pulmonary artery, and from the left ventricle to right ventricle respectively. $Pvcava$, PRV, and $PPart$ are the pressure in the vena cava, right ventricle and the pulmonary artery respectively. VRV is the volume of the right ventricle. $E_{rv}(t)$ is the elastance of the right ventricle and its plot is shown in Figure 2.5. During systole, $E_{rv}(t) = 0.45\ E_N(t)$ and during diastole, $E_{rv}(t) = 0.048$.

Left-to-Right Shunt:

$LtoRShunt = (PLV - PRV) / LtoRres$

where, $LtoRres$ is the resistance of the left-to-right ventricular shunt.

CHAPTER 4

METHODS

Computer simulation of the cardiovascular system is discussed for two different classes of problems:

(i) a forward problem which predicts the performance of the system for given parameter values under various conditions.

(ii) an inverse problem which estimates the values of unknown parameters and variables from the measured hemodynamic variables.

The former, the usual simulation, is used for understanding cardiovascular physiology in health and disease, and for investigating drug effects. Alternatively, the latter can be used to identify the cause of a disturbed state which has been created in the system.

The forward problem is solved by the iteration method. This iterative procedure was performed using a software package called VISSIM. It is a powerful simulation program based on the C programming language which provides complete visual and graphical work space for designing, and plotting models of dynamic systems. Integration of the equation was performed using a 2^{nd} order Runga-Kutta numerical integration algorithm. Computations were performed with a simulation time step size of 0.01 second.

The inverse problem was solved using a simulation of the diseased state, i.e. ventricular septal defect to identify the safe-limit left-to-right shunt resistance for different severity of the defect.

In the present study, simulations were performed in two parts:

(i) Simulation of the circulation under normal physiological conditions at rest to provide a baseline for comparison under other conditions, and also to establish a standard for the further study of the diseased state.

(ii) Simulation of the ventricular septal defect under the same physiological conditions, i.e. at the same pressures and volumes for each compartment. The effect of the shunt was then studied by varying the resistance of the shunt to identify the safe-limit resistance before the defect is considered life-threatening. These limits are rules of thumb or guidelines which appear in the clinical literature [4,6].

CHAPTER 5

RESULTS

Using the cardiovascular parameters given in Table 2.1, the variation of pressure and volume in each compartment for a normal human is obtained first. Figure 5.1 and Figure 5.2 shows the pressure and volume changes in left and right ventricle respectively. Figure 5.3 shows the relationship between pressure and volume in the left ventricle.

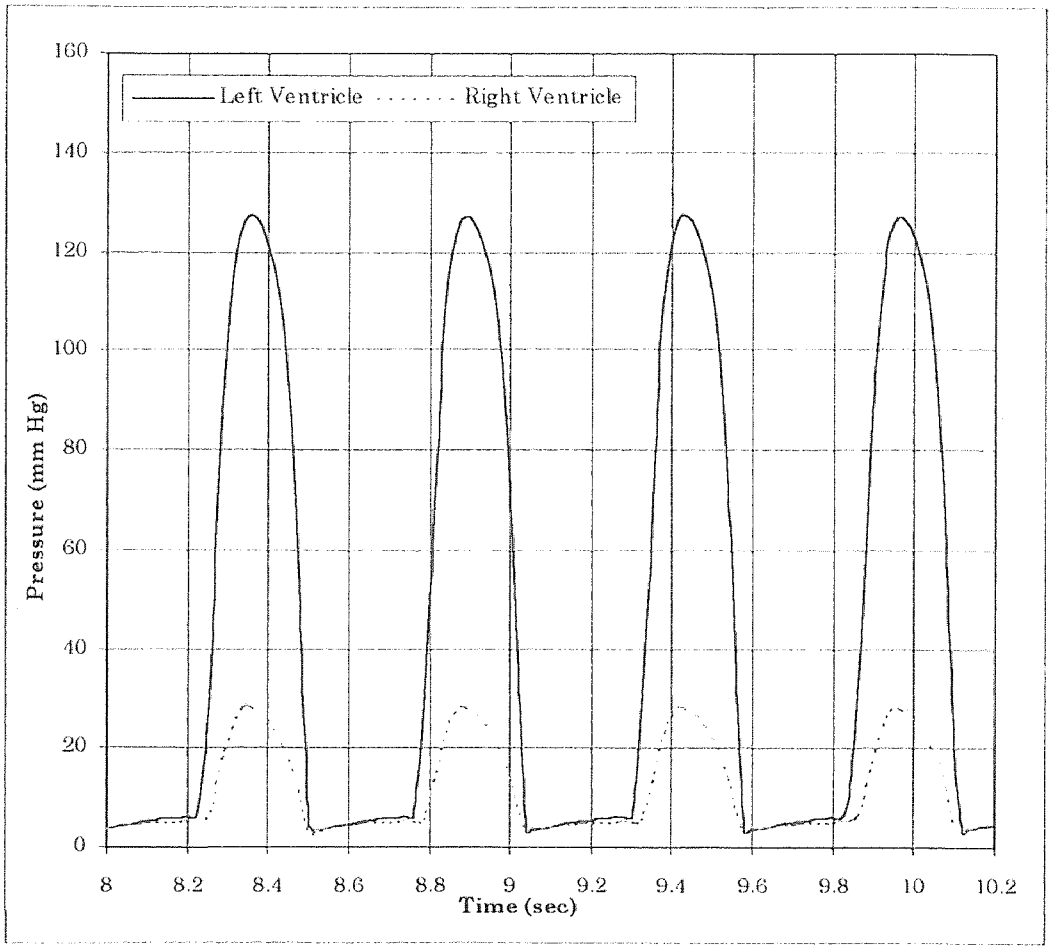

Figure 5.1. Pressure changes in left and right ventricles

The blood pressure in left and right ventricles generated by the simulation.

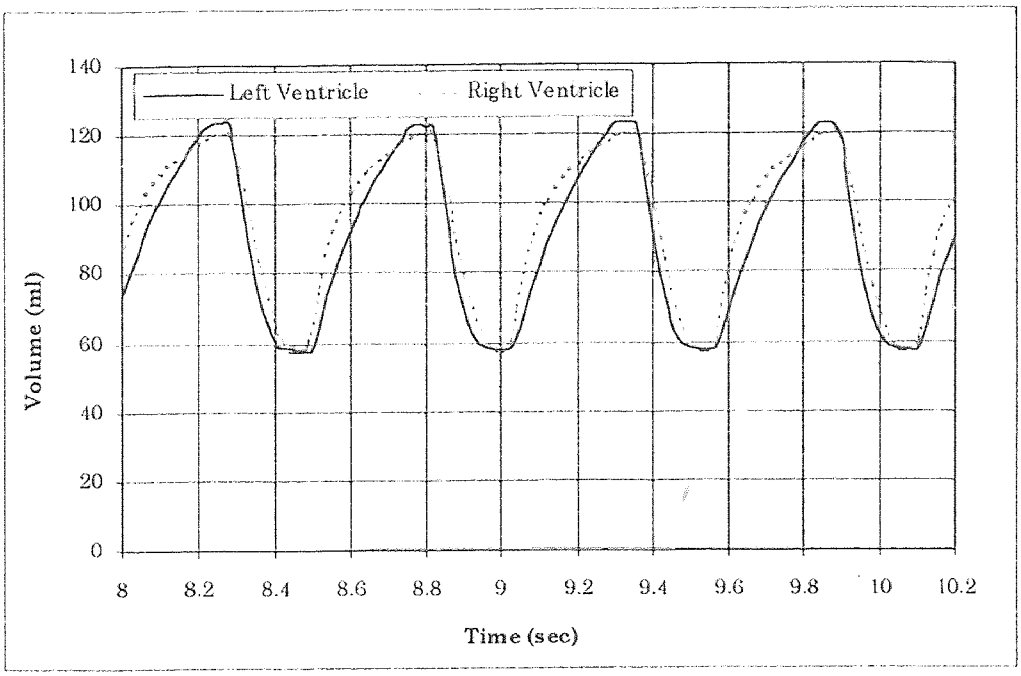

Figure 5.2. Volume changes in left and right ventricles.

Blood volume changes in left and right ventricles generated by the simulation.

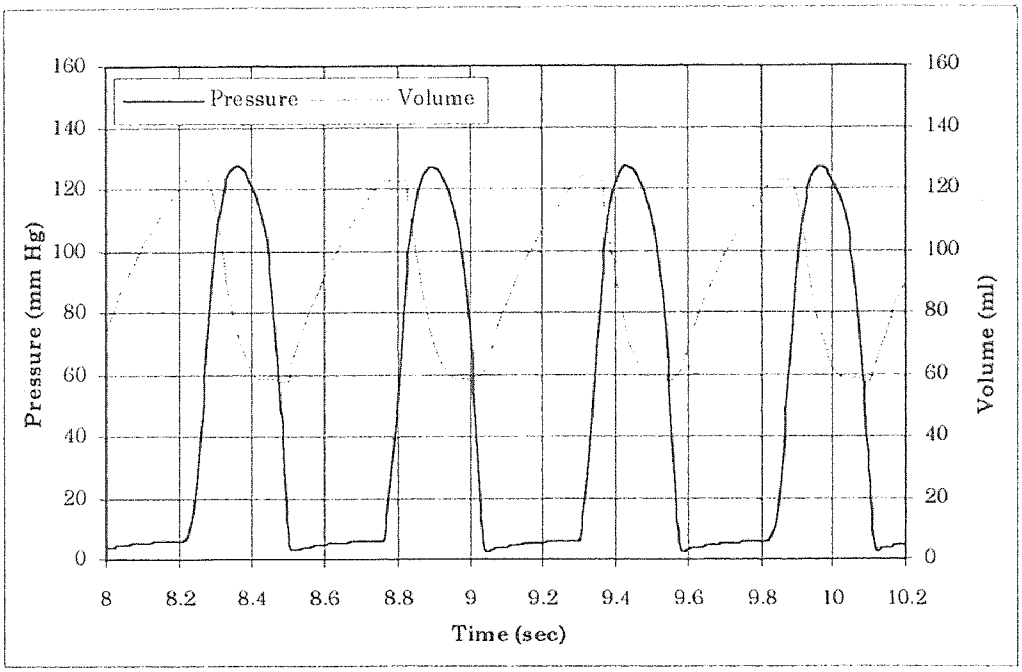

Figure 5.3. Pressure and Volume in Left Ventricle

Blood pressure and volume relationship in left ventricle during cardiac cycle generated by the simulation..

Figure 5.4 shows the pressure changes in the aorta, and Figure 5.5 is a comparison of blood flow in the pulmonary circulation, and the systemic circulation.

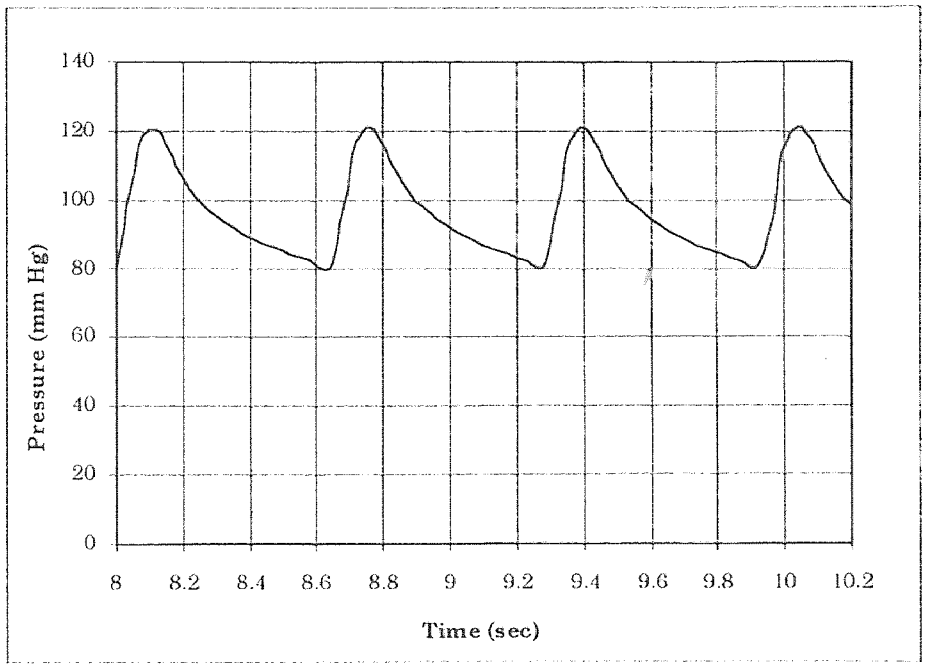

Figure 5.4. Pressure changes in aorta.

Blood pressure changes in aorta generated by the simulation.

A plot of intraventricular pressure versus volume for the left and right ventricles are shown in Figure 5.6 and Figure 5.7 respectively. These are used to calculate hemodynamic variables, such as stroke volume and cardiac output.

The stroke volume for the left ventricle is 67 ml. Cardiac output is 5025 ml/min. Total blood volume is 5023 ml. The pressure and volume ranges for each of the compartments of the model is shown in Table 5.1. The maximum pressure refers to the end systolic pressure and minimum to the end diastolic pressure. The maximum volume refers to the end diastolic volume and minimum volume refers to the end systolic volume.

Table 5.1. The range of blood pressure and volume in normal human at rest generated by the simulation.

Compartment	Pressure Range (mm Hg)	Volume Range (ml)
Left Heart	127.64 - 3.09	123.77 - 57.77
Aorta	121.23 - 80.69	135.77 - 110.44
Large Artery	101.24 - 78.46	131.40 - 114.89
Arterioles	83.11 - 73.51	191.45 - 175.44
Systemic Capillaries	12.89 - 12.79	464.16 - 462.69
Venules	8.47 - 8.44	451.69 - 451.04
Large Vein	8.04 - 7.99	2562.99 - 2557.40
Vena cava	6.69 - 5.22	444.23 - 412.84
Right Heart	28.49 - 2.66	120.80 - 57.55
Pulmonary Arteries	17.76 - 11.16	176.32 - 143.32
Pulmonary Capillaries	14.20 - 10.38	130.55 - 113.61
Pulmonary Veins	12.92 - 9.27	248.58 - 219.77

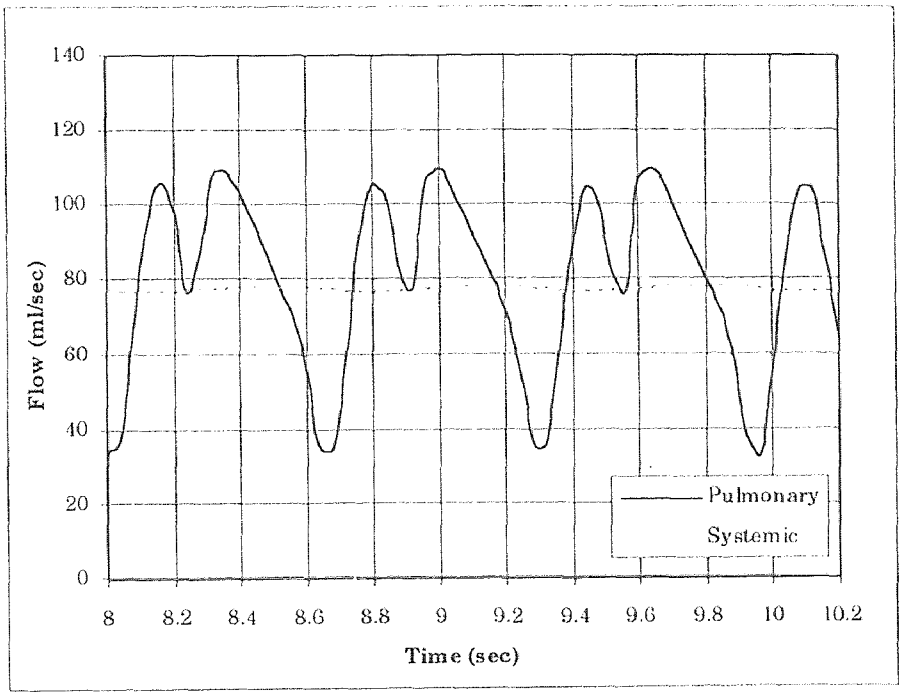

Figure 5.5. Flow in pulmonary and systemic circulation.

Comparison of flow in pulmonary and systemic circulation generated by the simulation.

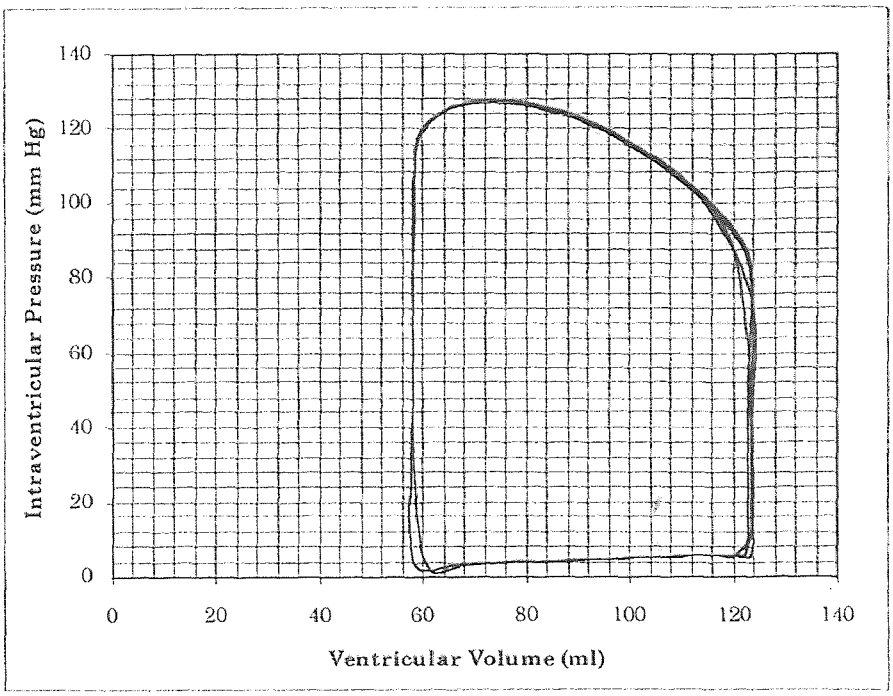

Figure 5.6. P-V plot for left ventricle.

Intraventricular pressure versus ventricular volume for left ventricle generated by the simulation.

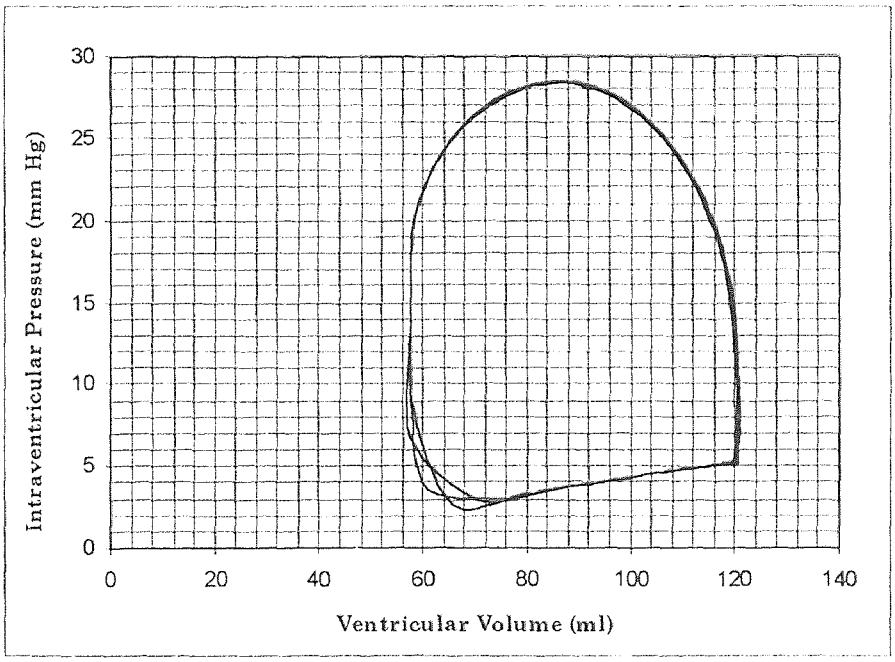

Figure 5.7. P-V plot for right ventricle

Intraventricular pressure versus ventricular volume for right ventricle generated by the simulation.

Figure 5.8 to Figure 5.20 shows plots of both left and right ventricles and the aorta for left-to-right shunt resistance of 10, 0.8, 0.6, 0.4, 0.3, 0.2, 0.1, 0.05, 0.02 (mmHg/ml/sec) respectively except for Figures 5.14, 5.15, 5.18 & 5.19. which shows the relationship between intraventricular pressure and ventricular volume for left-to-right shunt resistance of 0.2 and 0.05 for left and right ventricles. A plot of the shunt resistance versus the pulmonary to systemic flow ratio is shown in Figure 5.21a & Figure 5.21b and are summarized in Table 5.2.

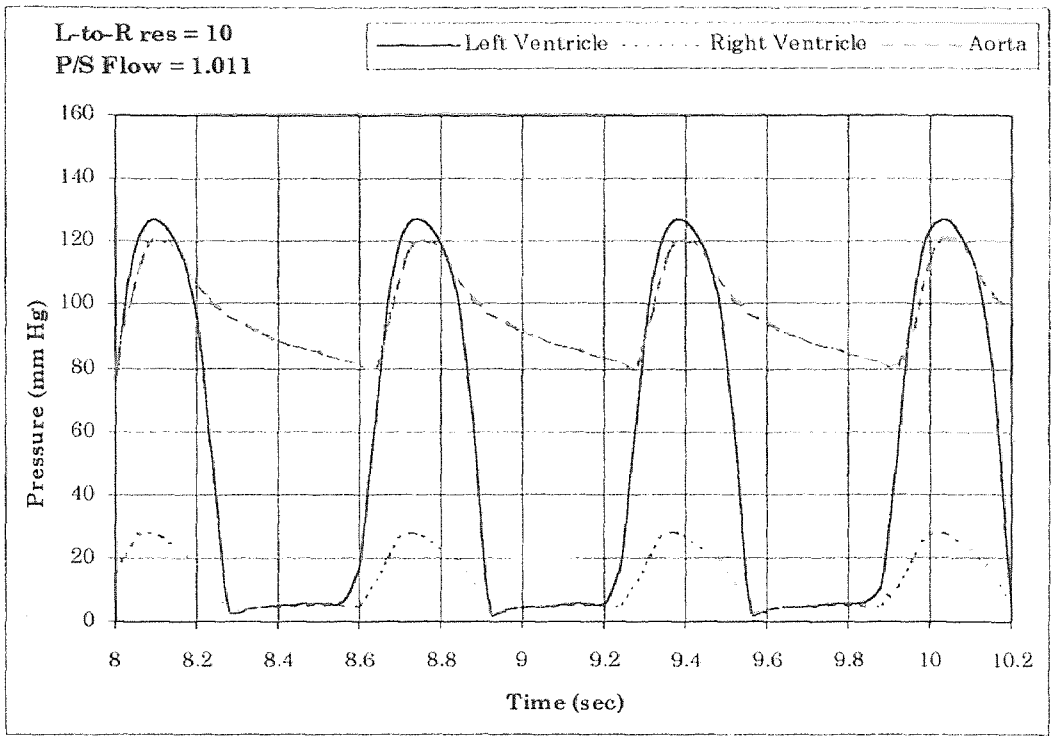

Figure 5.8. Pressure changes when L-to-R resistance equal to 10.

Left and right ventricular and aortic pressure in the circulation simulated by VSD model when the shunt resistance equal to 10 and the pulmonary to systemic flow ratio equal 1.011.

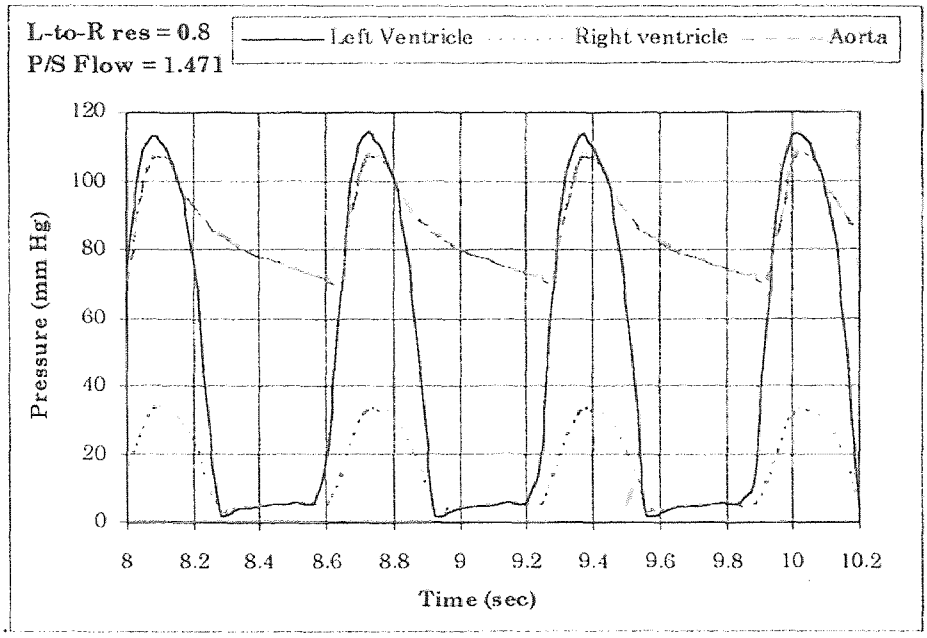

Figure 5.9. Pressure changes when L-to-R resistance equal to 0.8.

Left and right ventricular and aortic pressure in the circulation simulated by VSD model when the shunt resistance equal to 0.8 and the pulmonary to systemic flow ratio equal 1.471.

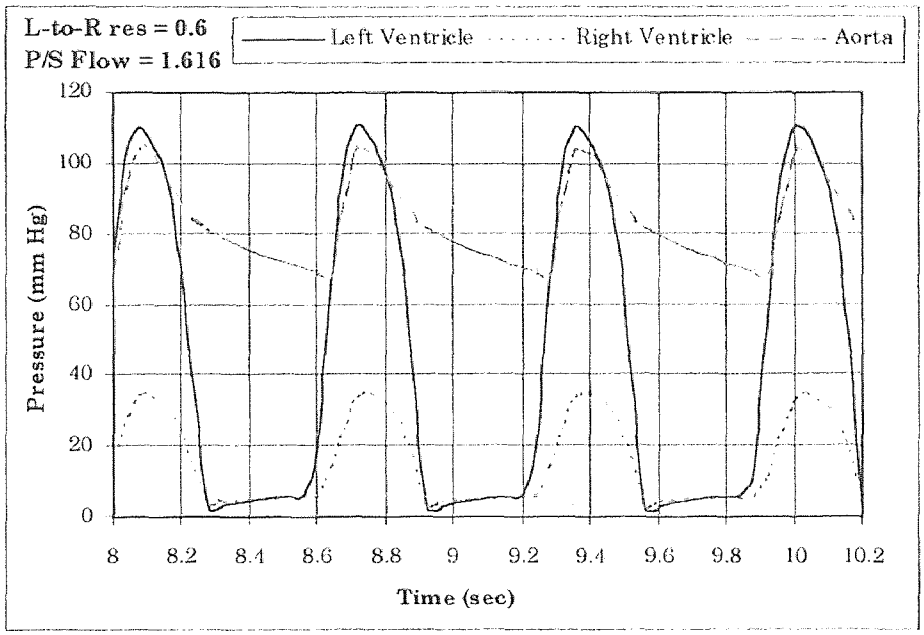

Figure 5.10. Pressure changes when L-to-R resistance equal to 0.6

Left and right ventricular and aortic pressure in the circulation simulated by VSD model when the shunt resistance equal to 0.6 and the pulmonary to systemic flow ratio equal 1.616

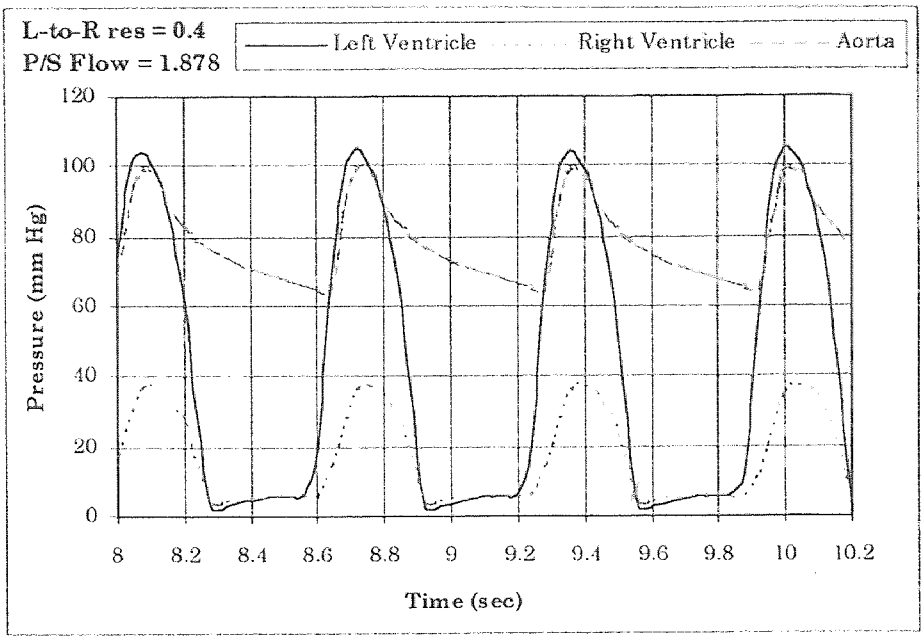

Figure 5.11. Pressure changes when L-to-R resistance equal to 0.4

Left and right ventricular and aortic pressure in the circulation simulated by VSD model when the shunt resistance equal to 0.4 and the pulmonary to systemic flow ratio equal 1.878

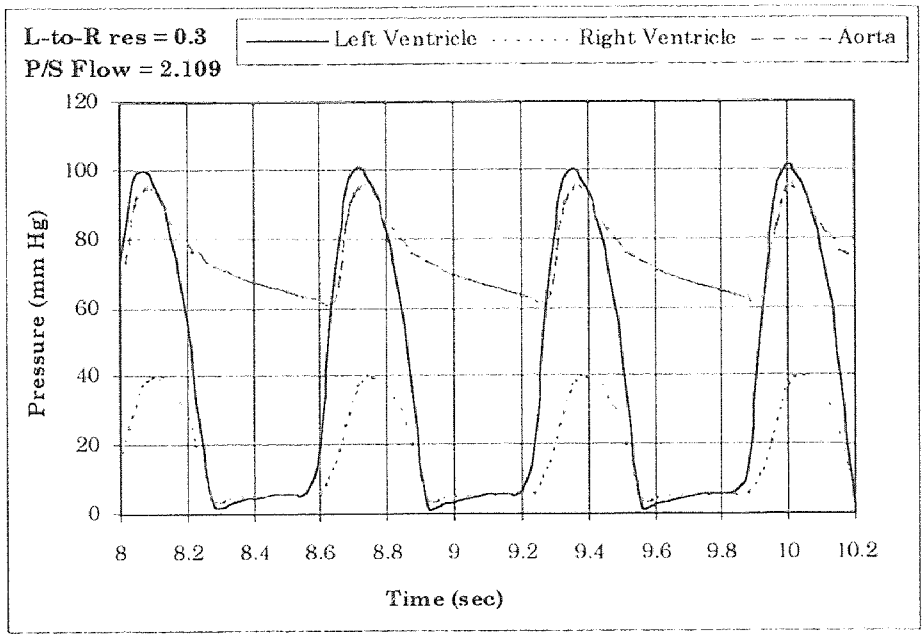

Figure 5.12 Pressure changes when L-to-R resistance equal to 0.3

Left and right ventricular and aortic pressure in the circulation simulated by VSD model when the shunt resistance equal to 0.3 and the pulmonary to systemic flow ratio equal 2.109

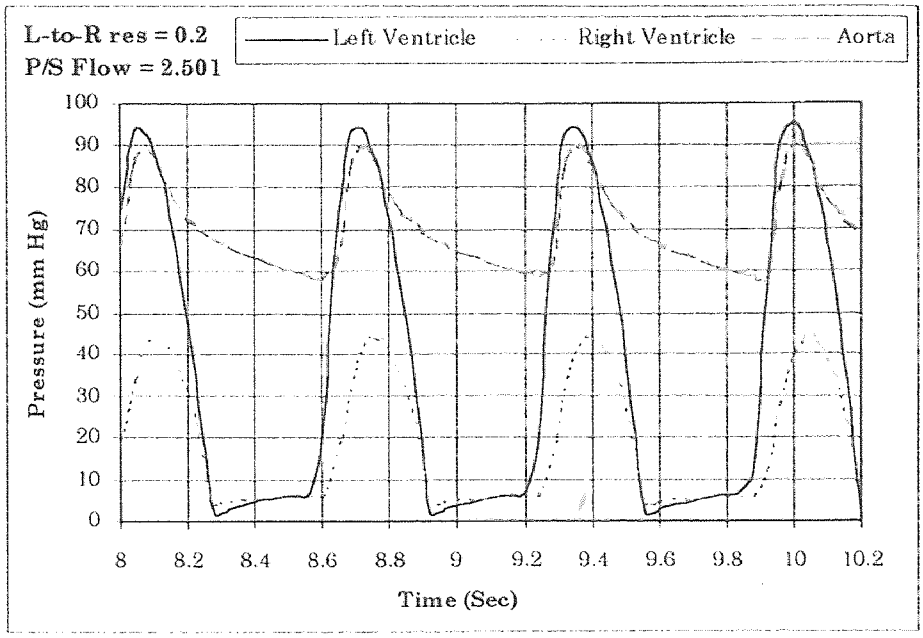

Figure 5.13 Pressure changes when L-to-R resistance equal to 0.2

Left and right ventricular and aortic pressure in the circulation simulated by VSD model when the shunt resistance equal to 0.2 and the pulmonary to systemic flow ratio equal 2.501

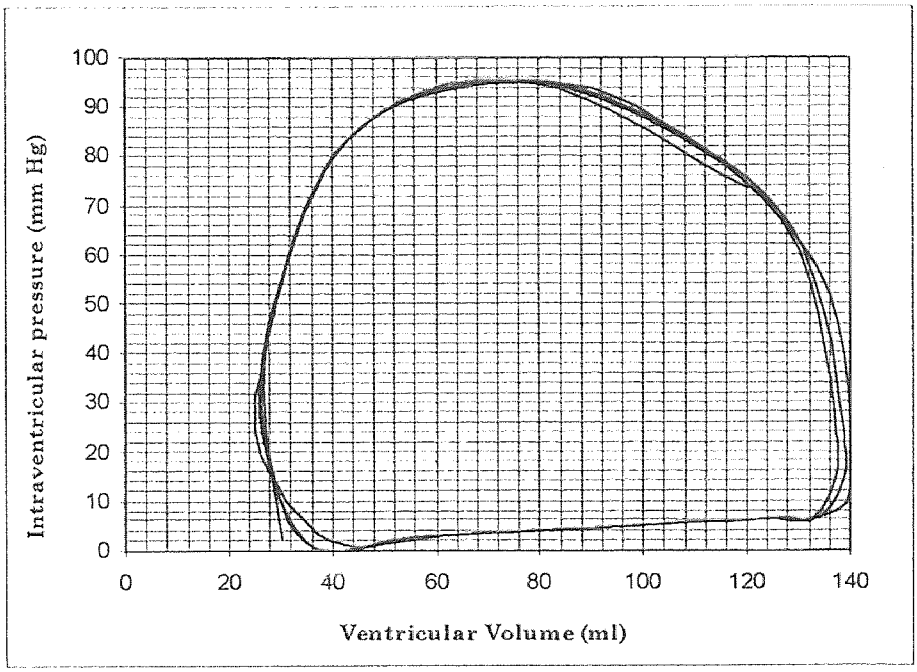

Figure 5.14. P-V plot for left ventricle when L-to-R resistance equal to 0.2.

Intraventricular pressure versus ventricular volume for left ventricle generated by the simulation.

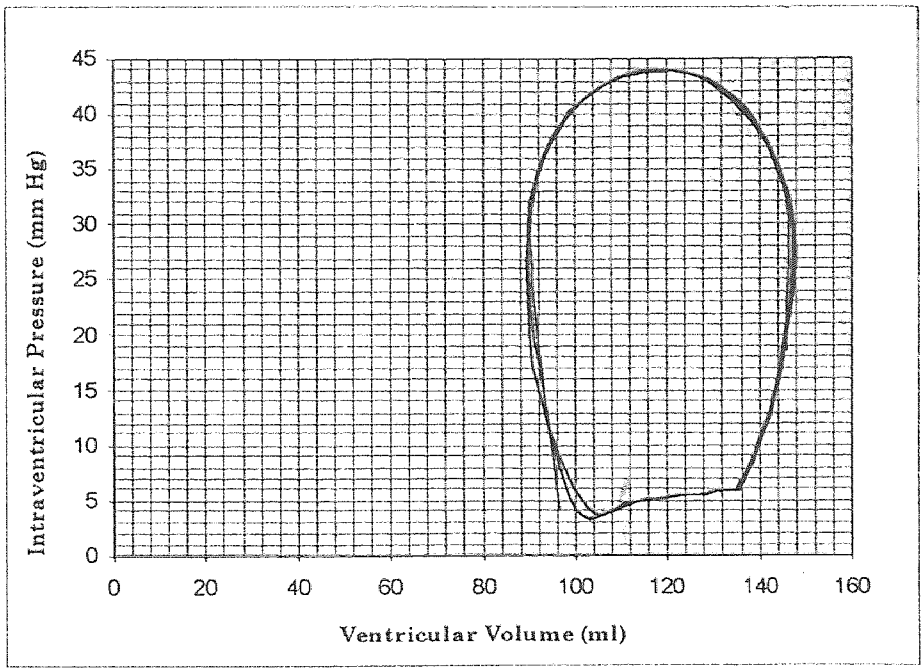

Figure 5.15. P-V plot for right ventricle when L-to-R resistance equal 0.2

Intraventricular pressure versus ventricular volume for right ventricle generated by the simulation.

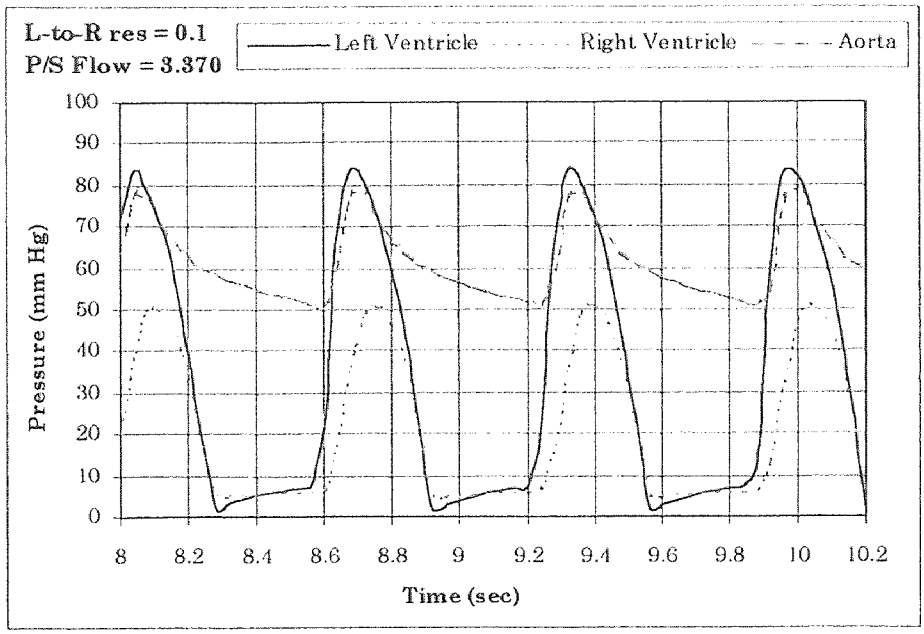

Figure 5.16 Pressure changes when L-to-R resistance equal to 0.1

Left and right ventricular and aortic pressure in the circulation simulated by VSD model when the shunt resistance equal to 0.1 and the pulmonary to systemic flow ratio equal 3.370

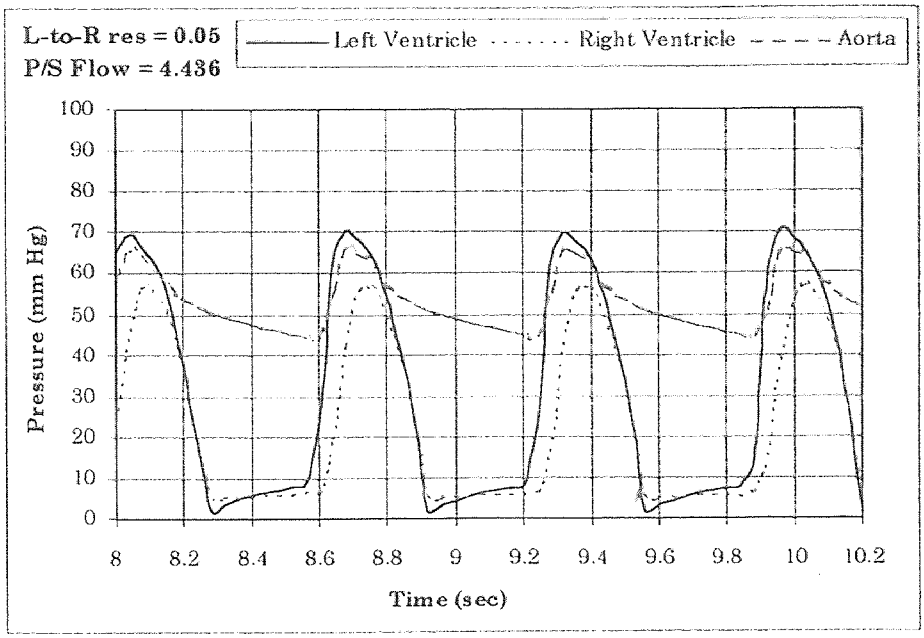

Figure 5.17 Pressure changes when L-to-R resistance equal to 0.05

Left and right ventricular and aortic pressure in the circulation simulated by VSD model when the shunt resistance equal to 0.05 and the pulmonary to systemic flow ratio equal 4.436

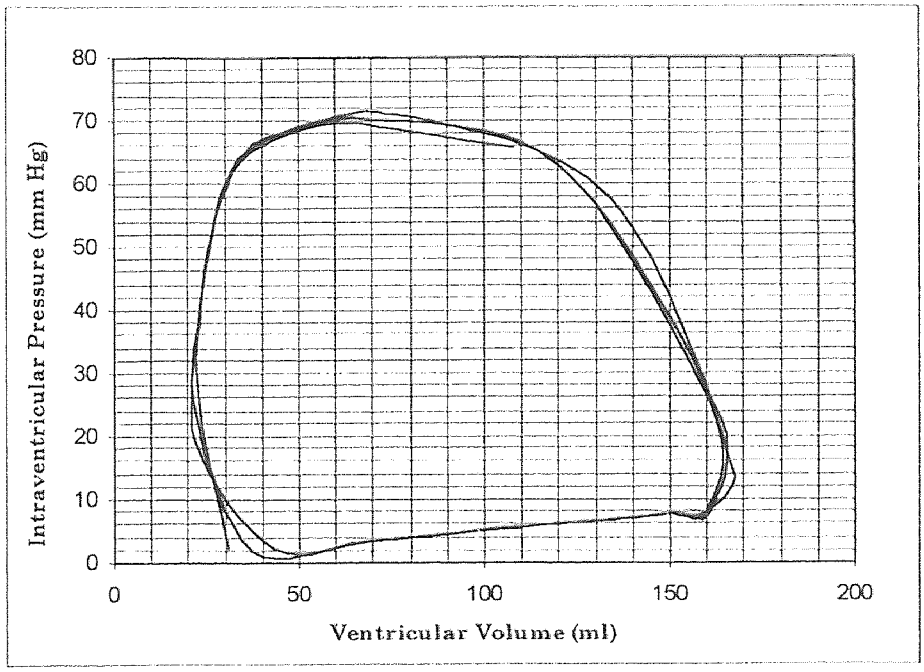

Figure 5.18. P-V plot for left ventricle when L-to-R resistance equal to 0.05.

Intraventricular pressure versus ventricular volume for left ventricle generated by the simulation

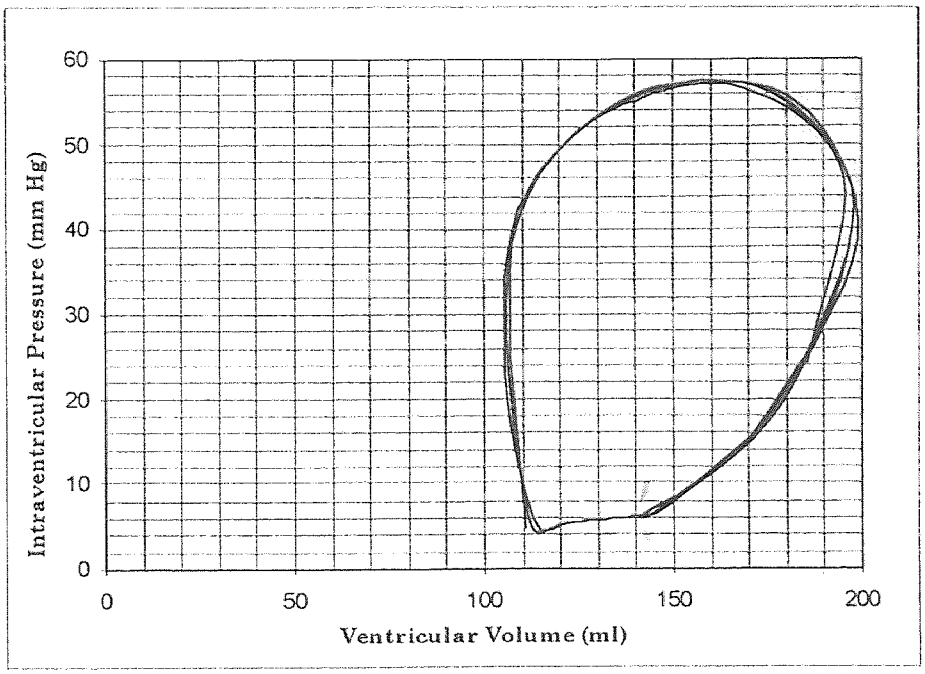

Figure 5.19. P-V plot for right ventricle when L-to-R resistance equal 0.05

Intraventricular pressure versus ventricular volume for right ventricle generated by the simulation.

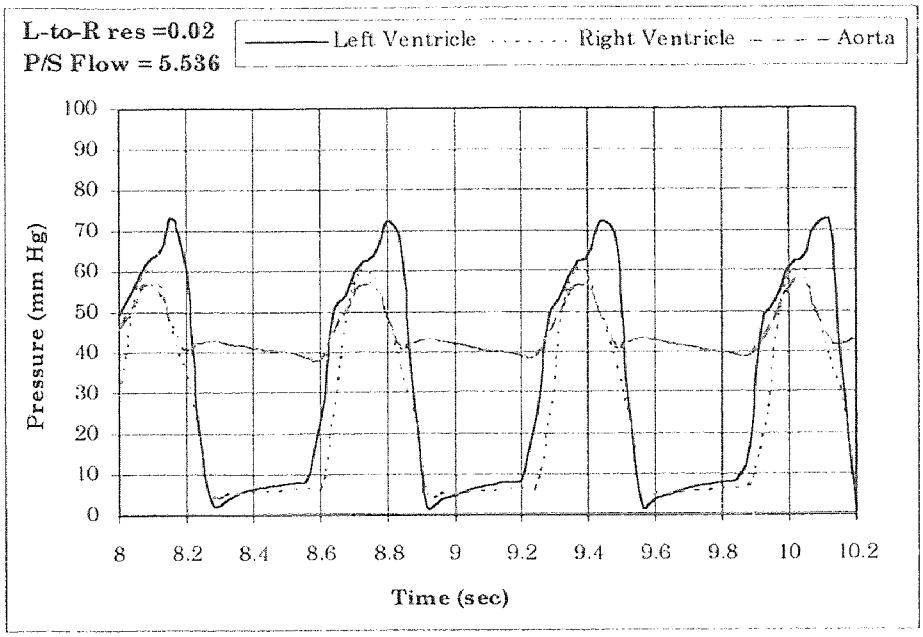

Figure 5.20 Pressure changes when L-to-R resistance equal to 0.02

Left and right ventricular and aortic pressure in the circulation simulated by VSD model when the shunt resistance equal to 0.02 and the pulmonary to systemic flow ratio equal 5.536

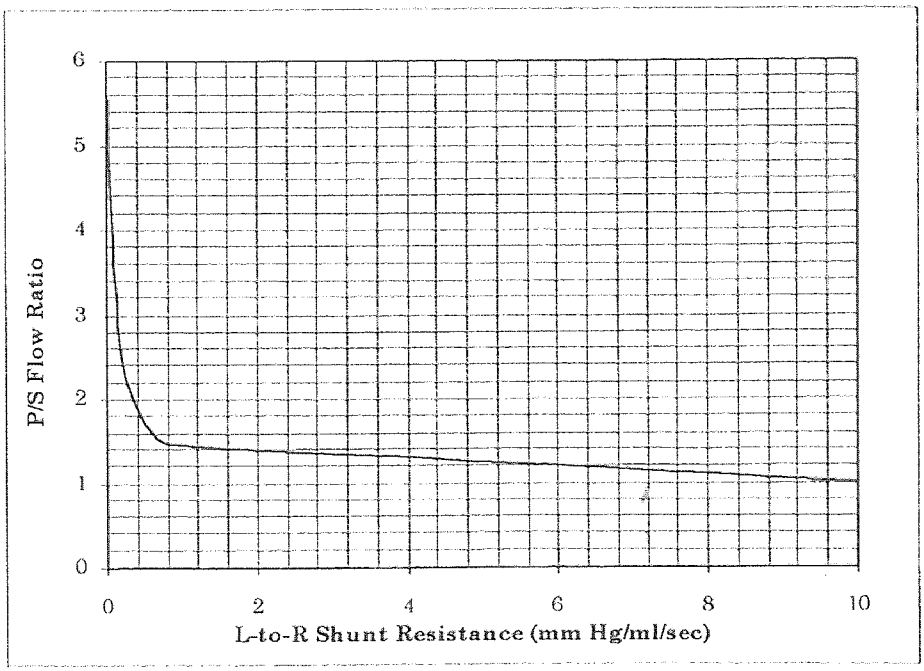

Figure 5.21a. Shunt resistance versus Pulmonary to Systemic flow ratio.

Plot of the pulmonary to systemic flow ratio versus the left-to-right shunt resistance based on data produced by simulation.

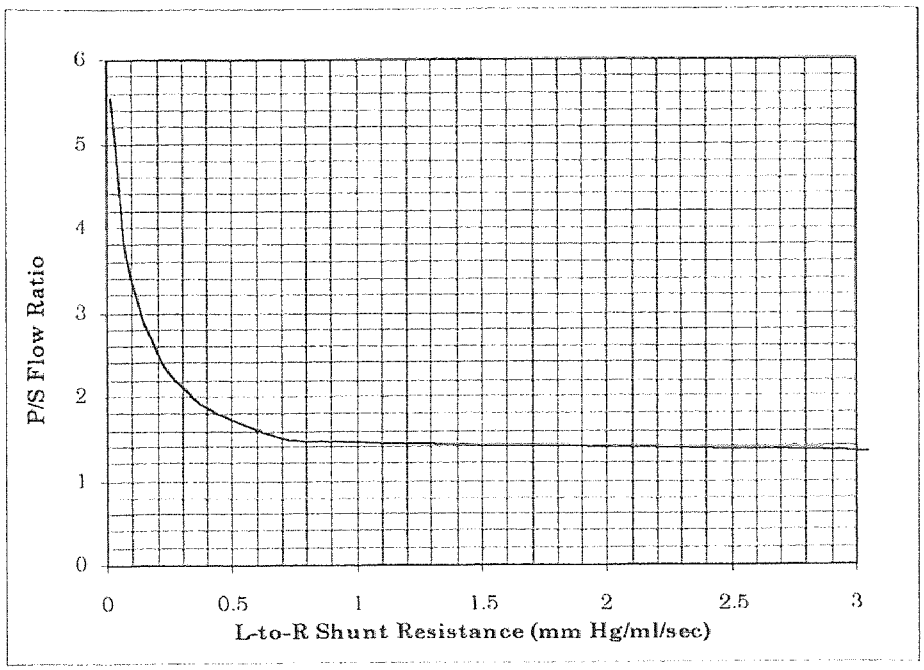

Figure 5.21b. Shunt resistance versus Pulmonary to Systemic flow ratio (magnified view).

Plot of the pulmonary to systemic flow ratio versus the left-to-right shunt resistance based on data produced by simulation.

Table 5.2 Values for the Pulmonary to Systemic Flow Ratio for different values for L-to-R shunt resistance.

L-to-R Shunt Resistance (mm Hg/ml/sec)	Averaged[1] Pulm. To Sys. Flow Ratio
10	1.011876
0.8	1.471771
0.6	1.616792
0.4	1.877877
0.3	2.109585
0.2	2.500983
0.1	3.370187
0.05	4.435901
0.02	5.53617

CHAPTER 6

DISCUSSION

6.1 Simulation of Cardiovascular System

The reliability of the parameter values is an important factor for the validity of a model itself. The parameters used in this model have produced simulations that are in close approximation with the experimentally measured values. The present cardiovascular model consists of twelve compartments covering the major components of the circulatory system. Each compartment has its characteristic resistance and compliance which produces a characteristic blood pressure and volume range. The unstressed volumes for each compartment were additionally fine tuned to achieve a match with the range of known data.

The ventricular pressure and volume are in good agreement with the literature values. The compliance of the ventricles were estimated using the Suga's elastance model, which is a good approximation of the actual compliances measured in the ventricular chambers of the heart.

The aortic pressure generated from the simulation ranges from 121.23 to 80.69 mm Hg, which are in good agreement with the aortic pressures measured in the human circulatory system [9].

The pressure/volume relationship for the left ventricles produces a stroke volume of approximately 67 ml as shown in Figure 5.6. The curve produced simulates the actual relationship very well.

Average values for the pressures in various segments of the cardiovascular system are shown in Figure 2.3. The range of pressures obtained from the simulation of the cardiovascular system for each compartment using the model

developed in this thesis are given in Table 5.1. The corresponding values are in good agreement with each other. A comparison of pressures in major compartment is shown in Table 6.1. Such an agreement in pressure and volume variation between reported measurements and the model output validates the model for use in the further study of disease conditions.

The validated model is then used to study ventricular septal defects which is the primary objective of this work.

Table 6.1 Simulation pressure data compared to literature values

	Pressure (mm Hg) *Simulation*	Pressure (mm Hg) *Literature*
Left Ventricle		
Systolic	127.64	90 - 140
End-diastolic	3.09	6 - 12
Aorta		
Systolic	121.23	90 - 140
Diastolic	80.69	70 - 90
Right Ventricle		
Systolic	28.49	20 - 30
End-diastolic	2.66	2 - 7
Vena Cava	6.69 - 5.22	2 - 8

6.2 Simulation of Ventricular Septal Defect

Ventricular septal defect originates from the ventricular septum. This defect is produced when a left-to-right shunt develops in the heart allowing the transfer of oxygenated blood back into the pulmonary circulation through back flow from the left ventricle to the right ventricle. Due to this back flow, the left ventricular pressure is reduced and the right ventricular pressure rises from their normal values. The reduced flow into the left ventricle makes the heart muscles work

harder to produce the desired cardiac output. The increased flow in the right ventricle causes an enlargement of the right ventricle which can be seen via echocardiography.

This defect is incorporated in the present cardiovascular model by introducing a parallel flow stream from the left ventricle to the right ventricle as shown in Figure 3.2. This parallel flow (left-to-right shunt) is assumed to have its own characteristic resistance to flow. This resistance is the determining factor for the severity of the defect. In other words, if the shunt resistance is low, more back flow will occur and the defect will be larger. A larger defect can be corrected only by surgery which is a complicated procedure with a high mortality (about 15-25%) [6]. On the other hand, small defects rarely need any surgical procedure other than prophylaxis, if bacterial endocarditis (an infection of the heart muscle due to the back flow to the lungs) occurs[11]. Thus, it is important to identify when a defect is large and when it is small.

The severity of the defect also has a direct relationship on the pulmonary to systemic flow ratio in the circulation. If this ratio is above 2:1, the defect is considered a large defect [4]. In the present model, when this ratio is about 2.1:1, the aortic pressure falls within the range of 100 mm Hg to about 67 mm Hg as shown in Figure 5.11. This drop in pressure from 120 to 100 mm Hg causes the stroke volume to increase and in turn increases the work load on the heart.

The effect of the shunt resistance on the pulmonary to systemic flow ratio is quantified in the present study. The ratios were calculated at different values of the shunt resistance (Table 5.2) and were plotted as shown in Figure 5.16a and Figure 5.16b. From Figure 5.16b, the safe-limit resistance (defined as when the pulmonary to systemic flow ratio is $\leq$ 2:1) after which the defect is considered large is 0.33

mmHg/ml/sec. This is quite high as compared with the resistances of the pulmonary valve (0.0333 mmHg/ml/sec), mitral valve (0.0334 mmHg/ml/sec) and aortic valve (0.02 mmHg/ml/sec).

For a simple ventricular defect, the surgical procedure (especially in pediatric cases) was to put a metal band around the pulmonary artery to increase its hemodynamic resistance and reduce the work load on the heart. The present model simulates this perfectly. The pressure/volume relationship for the condition when the shunt resistance is 0.3 mmHg/ml/sec is shown in Figure 6.1a and Figure 6.1b in left and right ventricles respectively. The effect of pulmonary artery banding, i.e. increased pulmonary resistance on the pressure/volume relationship is shown in Figure 6.2a and Figure 6.2b for left and right ventricles respectively. The stroke volume and hence the stroke work has been reduced by pulmonary artery banding as shown in Figure 6.1a to Figure 6.2b. It is clear from the figures that the model simulates the ventricular septal defect closely. Thus, this model can be used as a tool to determine the resistance needed at the pulmonary artery to achieve a desired stroke volume (and hence cardiac output).

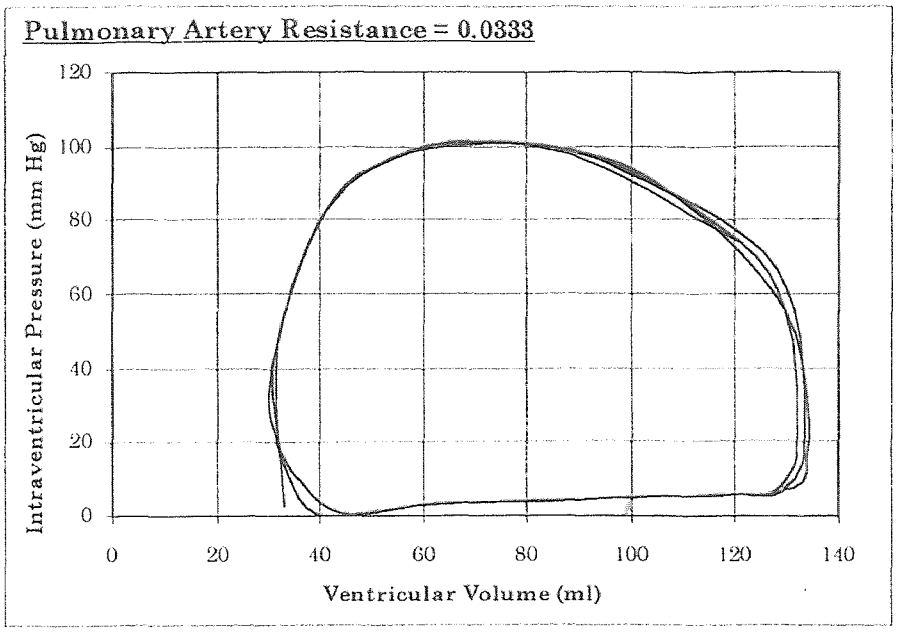

Figure 6.1a. Pressure/Volume Relationship of Left ventricle

Blood pressure/volume relationship for the left ventricle generated by the simulation at left-to-right shunt resistance = 0.3 and pulmonary artery resistance = 0.0333

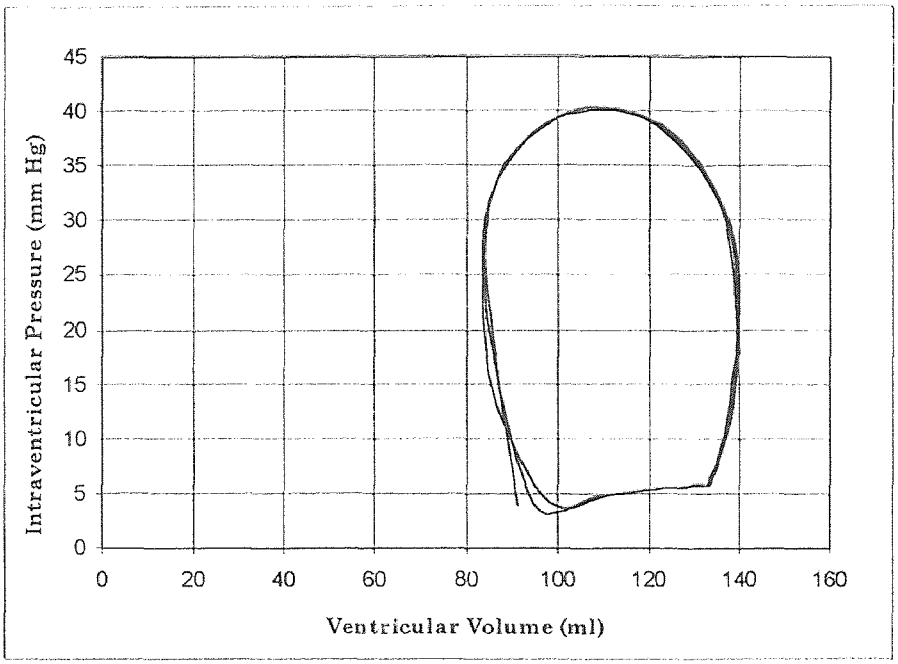

Figure 6.1b. Pressure/Volume Relationship of Right ventricle

Blood pressure/volume relationship for the right ventricle generated by the simulation at left-to-right shunt resistance = 0.3 and pulmonary artery resistance = 0.0333

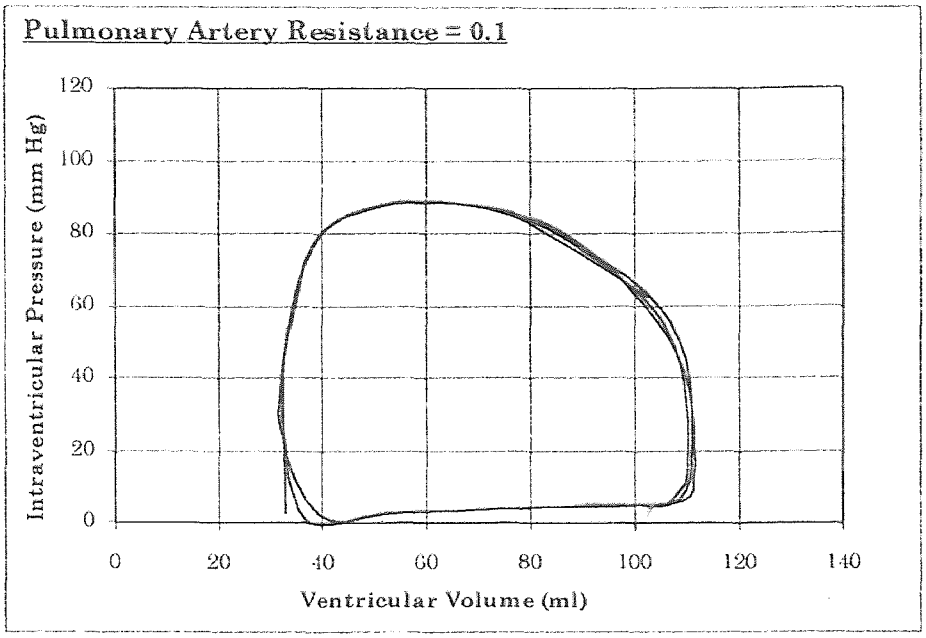

Figure 6.2a Pressure/Volume Relationship of Left ventricle

Blood pressure/volume relationship for the left ventricle generated by the simulation at left-to-right shunt resistance = 0.3 and pulmonary artery resistance = 0.1. This increased pulmonary artery resistance simulates the surgical procedure known as pulmonary artery banding.

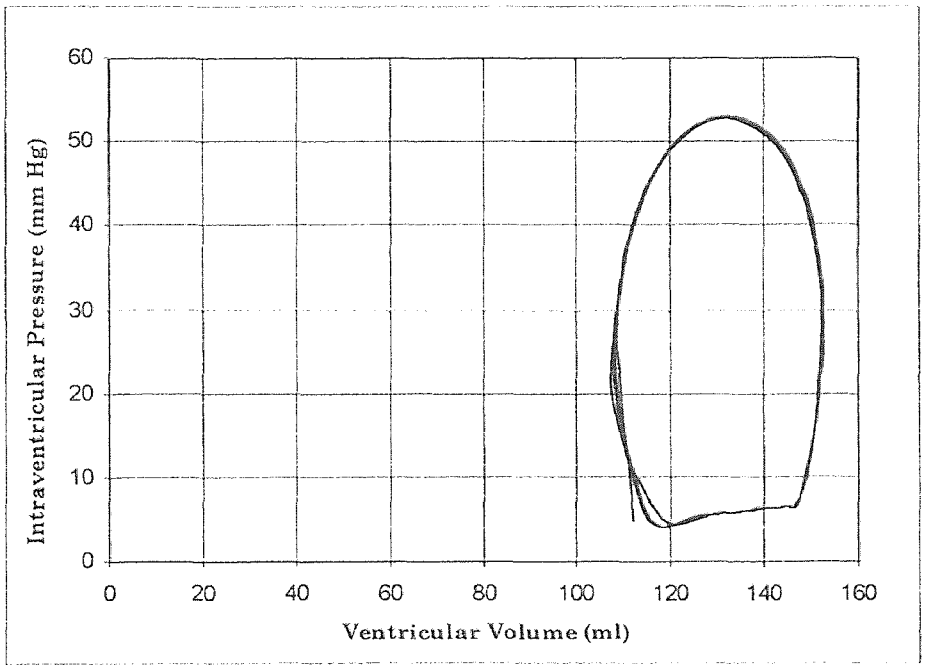

Figure 6.2b Pressure/Volume Relationship of Right ventricle

Blood prossure/volume relationship for the right ventricle generated by the simulation at left-to-right shunt resistance = 0.3 and pulmonary artery resistance = 0.1. This increased pulmonary artery resistance simulates the surgical procedure known as pulmonary artery banding.

CHAPTER 7

CONCLUSIONS

Despite the simplifications, the model used in this study has shown good agreement with the clinical and experimental data under a wide variety of conditions. The present model provides a simple and quite accurate understanding of the cardiac hemodynamics of ventricular septal defect. The shunt resistance regulates the severity of the defect which portrays the cardinal feature of the ventricular septal defect, i.e. the size of defect.

It was observed in the model that the left ventricular pressure falls and the right ventricular pressure rises as the septal defect gets larger. It was also observed that when the pulmonary artery resistance is increased, the stroke volume of the left ventricle is regulated. The model, thus, suggests that in case of simple ventricular septal defect, pulmonary artery banding offers a low-risk treatment for smaller defects. Hence, the model can be used as a guiding tool for analyzing ventricular septal defects and selecting the proper banding size for surgical treatment of small defects.

CHAPTER 8

LIMITATIONS OF THE MODEL

The model predicts the normal hemodynamics of the cardiovascular system and of a particular set of disease conditions. However, the model include the effects of auto regulation and oxygen-transport. These features were not necessary to study the hemodynamic changes in ventricular septal defects.

CHAPTER 9

RECOMMENDATIONS FOR FURTHER STUDY

The present model has the capabilities to study the hemodynamics of some other congenital diseases. For example, patent ductus arteriosus, or mitral stenosis, etc. For further study, this model will be used to study other congenital diseases.

REFERENCES

1. Barnea, O. "Mathematical analysis of coronary autoregulation and vascular reserve in closed-loop circulation". *Comput, & Biomed Res.* 27:263-275;1994.

2. Bergel, D.H. *Cardiovascular Fluid Dynamics.* Vol.1. Academic Press, New York, 1972.

3. Berne, R.M. and Levy, M.N. *Principle of Physiology.* Part iv:, The C.V. Mosby Company, 188-313. St. Lois, MO, 1990.

4. Cheitlin, M.D., Sokolow, M. and McIlroy, M.B. *Clinical Cardiology.* 6th ed. Appleton & Lange Medical Publishers, Norwalk, CT, 1993.

5. Guyton, A.C. *Text book of Medical Physiology.* 8th ed. W.B. Saunders Company, Philadelphia, PA 1991.

6. Hathaway, W.E., Hay Jr., W.W., Groothuis, J.R. and Paisley, J.W. *Current Pediatric Diagnosis & Treatment.* 11th ed. Appleton & Lange Medical Publishers, Norwalk, CT, 1993.

7. Johnson, L. R. *Essentials of Medical Physiology.* Raven Press, New York, 1992.

8. Julian, D.G. *Cardiology.* Bailliere Tindall, London, 1973.

9. Lentner, C. "Heart and Circulation". *Geigy Scientific Tables.* Vol.5. CIBA-GEIGY Limited, Basel. 1990.

10. McLead, J., "PHYSBE, a physiological simulation benchmark experiment". *Simulation.* Vol. 7, pp. 324-329, December 1966.

11. Merenstein, G.B., Kaplan, D.W. and Rosenberg, A.A. *Handbook of Pediatrics.* 16th ed. Appleton & Lange Medical Publishers, Norwalk, CT, 1991.

12. Netter, F.H. "Heart". *The CIBA Collection of Medical Illustrations.* Vol. 5, Colorpress, New York, 1978.

13. Rideout, V. *Mathematical and Computer Modeling of Physiological Systems.* Prentice Hall, Englewood Cliffs, NJ, 1991.

14. Shroff, S.G., Janicki, J.S. and Weber, K.T. "Left ventricular systolic dynamics in terms of its chamber mechanical properties". *Am. J. Physiol.* 245:H1110-124;1983.

15. Strandness, D.E., and Sumner, D.S. *Hemodynamics for Surgeons.* Grune & Stratton Publishers, New York, 1975.

16. Suga, H, and Sagawa, K. "Instantaneous pressure-volume relationships and their ratio in the excised, supported canine left ventricle". *Circ. Res.* 35:117-126;1974.

17. Tsuruta, H., Sato, T., Shirataka, M. and Ikeda, N. "Mathematical model of cardiovascular mechanics of diagnostic analysis and treatment of heart failure: Part 1 model description and theoretical analysis". *Med. & Bio. Engg. & Comput.* 32:3-11;1994.

18. Wenink, A.C.G. Oppenheimer-Dekker, A. and Moulaert, A.J. *The Ventricular Septum of the Heart.* Kluwer Academic Publishers Group, Netherlands, 1981.